24th International Workshop on ECR Ion Sources (ECRIS'20)

ECRIS 2020

28-30 September 2020

INFN LNS
Istituto Nazionale di Fisica Nucleare
Laboratori Nazionali del Sud

ADVANCEMENTS IN SELF-CONSISTENT MODELING OF TIME- AND SPACE-DEPENDENT PHENOMENA IN ECRIS PLASMA

Angelo Pidatella, David Mascali, Bharat Mishra, Eugenia Naselli, Giuseppe Torrisi, *INFN-LNS, Catania, Italy*
Alessio Galatà, *INFN-LNL, Legnaro, Italy*

INTRODUCTION

GOAL: Bridge the gap between theoretical and experimental study of **space-dependent** and **time-dependent** electron/ion properties/**phenomena** in ECR plasmas

See talk from (September 28):

- R. Ràcz: *Imaging in X-ray Ranges to Locally Investigate the Effect of the Two-Close-Frequency Heating in ECRIS Plasmas*
- E. Naselli: *High Resolution X-ray Imaging as a Powerful Diagnostics Tool to Investigate ECRIS Plasma Structure and Confinement Dynamics*

INTRODUCTION

GOAL: Bridge the gap between theoretical and experimental study of **space-dependent** and **time-dependent** electron/ion properties/**phenomena** in ECR plasmas

Examples:

SPACE: particles confinement dynamics, reaction rates for electromagnetic emissions, ion CSD

TIME: kinetic instabilities, plasma turbulences, fast transients, EC MASER instability

See talk from (September 28):

- R. Ràcz: *Imaging in X-ray Ranges to Locally Investigate the Effect of the Two-Close-Frequency Heating in ECRIS Plasmas*
- E. Naselli: *High Resolution X-ray Imaging as a Powerful Diagnostics Tool to Investigate ECRIS Plasma Structure and Confinement Dynamics*

INTRODUCTION

GOAL: Bridge the gap between theoretical and experimental study of **space-dependent** and **time-dependent** electron/ion properties/**phenomena** in ECR plasmas

Examples:
SPACE: particles confinement dynamics, reaction rates for electromagnetic emissions, ion CSD
TIME: kinetic instabilities, plasma turbulences, fast transients, EC MASER instability

THE EXPERIMENTAL SURVEY

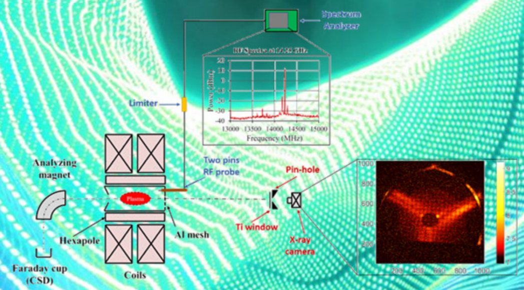

See talk from (September 28):
- R. Ràcz: *Imaging in X-ray Ranges to Locally Investigate the Effect of the Two-Close-Frequency Heating in ECRIS Plasmas*
- E. Naselli: *High Resolution X-ray Imaging as a Powerful Diagnostics Tool to Investigate ECRIS Plasma Structure and Confinement Dynamics*

INTRODUCTION

GOAL: Bridge the gap between theoretical and experimental study of **space-dependent** and **time-dependent** electron/ion properties/**phenomena** in ECR plasmas

Examples:
SPACE: particles confinement dynamics, reaction rates for electromagnetic emissions, ion CSD
TIME: kinetic instabilities, plasma turbulences, fast transients, EC MASER instability

THE EXPERIMENTAL SURVEY

SPACE-RESOLVED PLASMA STUDY

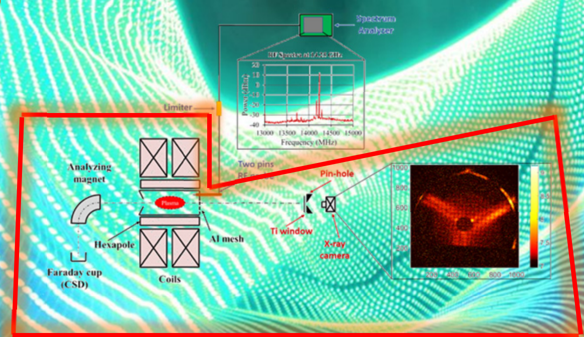

See talk from (September 28):
- R. Ràcz: *Imaging in X-ray Ranges to Locally Investigate the Effect of the Two-Close-Frequency Heating in ECRIS Plasmas*
- E. Naselli: *High Resolution X-ray Imaging as a Powerful Diagnostics Tool to Investigate ECRIS Plasma Structure and Confinement Dynamics*

INTRODUCTION

GOAL: Bridge the gap between theoretical and experimental study of **space-dependent** and **time-dependent** electron/ion properties/**phenomena** in ECR plasmas

Examples:
SPACE: particles confinement dynamics, reaction rates for electromagnetic emissions, ion CSD
TIME: kinetic instabilities, plasma turbulences, fast transients, EC MASER instability

THE EXPERIMENTAL SURVEY

SPACE-RESOLVED PLASMA STUDY

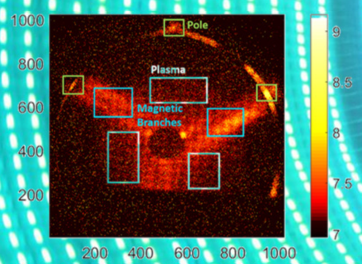

Space-resolved soft X-Ray imaging: monitoring confinement dynamics and plasma structure

E. Naselli *et al.* (2019), 10.1088/1748-0221/14/10/C10008

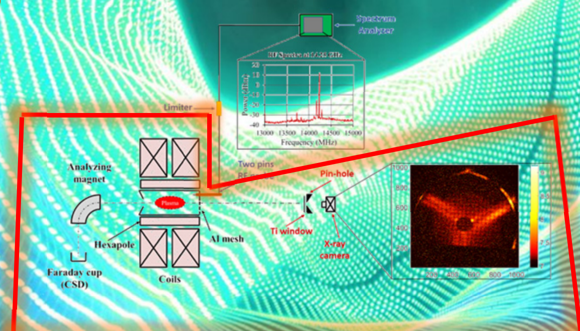

See talk from (September 28):
- R. Ràcz: *Imaging in X-ray Ranges to Locally Investigate the Effect of the Two-Close-Frequency Heating in ECRIS Plasmas*
- E. Naselli: *High Resolution X-ray Imaging as a Powerful Diagnostics Tool to Investigate ECRIS Plasma Structure and Confinement Dynamics*

INTRODUCTION

GOAL: Bridge the gap between theoretical and experimental study of **space-dependent** and **time-dependent** electron/ion properties/**phenomena** in ECR plasmas

Examples:
SPACE: particles confinement dynamics, reaction rates for electromagnetic emissions, ion CSD
TIME: kinetic instabilities, plasma turbulences, fast transients, EC MASER instability

THE EXPERIMENTAL SURVEY

SPACE-RESOLVED PLASMA STUDY

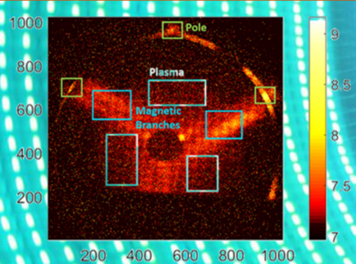

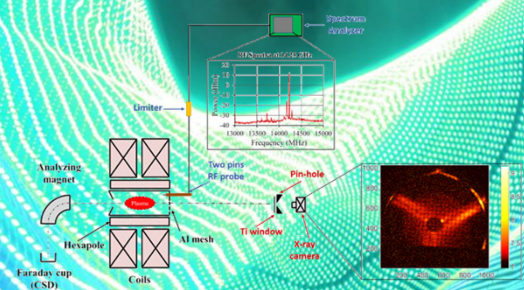

Space-resolved soft X-Ray imaging: monitoring confinement dynamics and plasma structure

E. Naselli *et al.* (2019), 10.1088/1748-0221/14/10/C10008

See talk from (September 28):
- R. Ràcz: *Imaging in X-ray Ranges to Locally Investigate the Effect of the Two-Close-Frequency Heating in ECRIS Plasmas*
- E. Naselli: *High Resolution X-ray Imaging as a Powerful Diagnostics Tool to Investigate ECRIS Plasma Structure and Confinement Dynamics*

INTRODUCTION

GOAL: Bridge the gap between theoretical and experimental study of **space-dependent** and **time-dependent** electron/ion properties/**phenomena** in ECR plasmas

Examples:
SPACE: particles confinement dynamics, reaction rates for electromagnetic emissions, ion CSD
TIME: kinetic instabilities, plasma turbulences, fast transients, EC MASER instability

THE EXPERIMENTAL SURVEY

SPACE-RESOLVED PLASMA STUDY

TIME-RESOLVED PLASMA STUDY

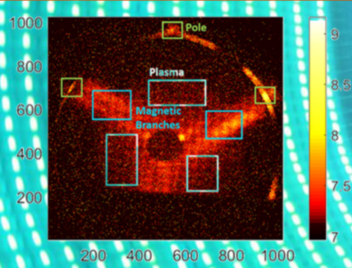

Space-resolved soft X-Ray imaging: monitoring confinement dynamics and plasma structure

E. Naselli *et al.* (2019), 10.1088/1748-0221/14/10/C10008

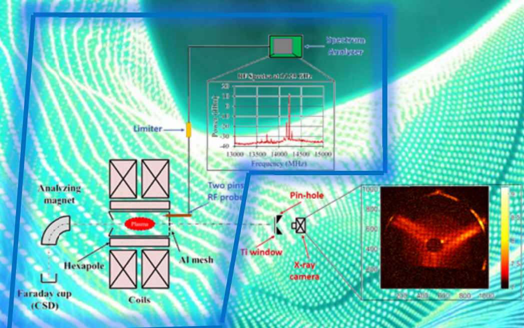

See talk from (September 28):
- R. Ràcz: *Imaging in X-ray Ranges to Locally Investigate the Effect of the Two-Close-Frequency Heating in ECRIS Plasmas*
- E. Naselli: *High Resolution X-ray Imaging as a Powerful Diagnostics Tool to Investigate ECRIS Plasma Structure and Confinement Dynamics*

INTRODUCTION

GOAL: Bridge the gap between theoretical and experimental study of **space-dependent** and **time-dependent** electron/ion properties/**phenomena** in ECR plasmas

Examples:
SPACE: particles confinement dynamics, reaction rates for electromagnetic emissions, ion CSD
TIME: kinetic instabilities, plasma turbulences, fast transients, EC MASER instability

THE EXPERIMENTAL SURVEY

SPACE-RESOLVED PLASMA STUDY

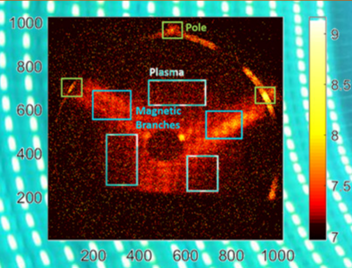

Space-resolved soft X-Ray imaging: monitoring confinement dynamics and plasma structure

E. Naselli *et al.* (2019), 10.1088/1748-0221/14/10/C10008

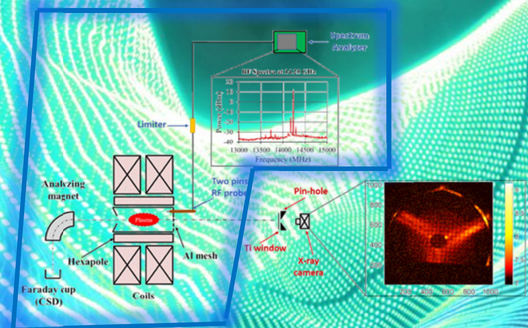

TIME-RESOLVED PLASMA STUDY

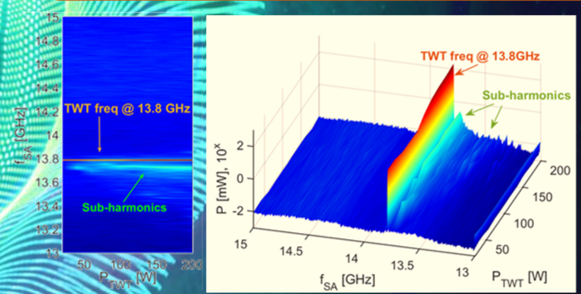

Time-averaged single-frequency spectral evolution of the RF-probe detected signal vs. pumping wave power, with sub-harmonics generation already evident at around 40 W

E. Naselli *et al.*, PSST 28 (2019) 085021

See talk from (September 28):
- R. Ràcz: *Imaging in X-ray Ranges to Locally Investigate the Effect of the Two-Close-Frequency Heating in ECRIS Plasmas*
- E. Naselli: *High Resolution X-ray Imaging as a Powerful Diagnostics Tool to Investigate ECRIS Plasma Structure and Confinement Dynamics*

ECR PLASMA ANISOTROPICITY

- Wave-to-particle coupling: heating process via electron cyclotron resonance (ECR)
  - RF guided wave + **multimodal structure**: highly **inhomogeneous**, **space-dependent electric field**

- **Space-dependent** and **highly-inhomogenous magnetic field** profile: plasma trapping + electron gyration

- **RESULTS: closed ECR surface for wave-particle coupling and heating**
- **RESULTS : space-dependent power transfer depending on electric field profile**

$$\omega = \omega_c = \frac{eB(r)}{m}$$

$$P \propto E(r)^2$$

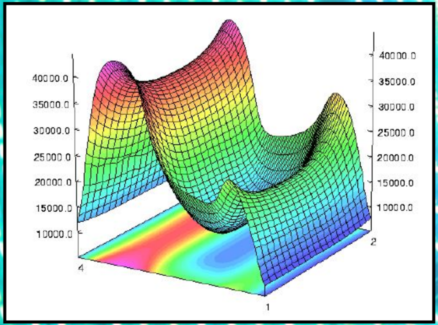

B-field profile as superposition of min-B and hexapole structures

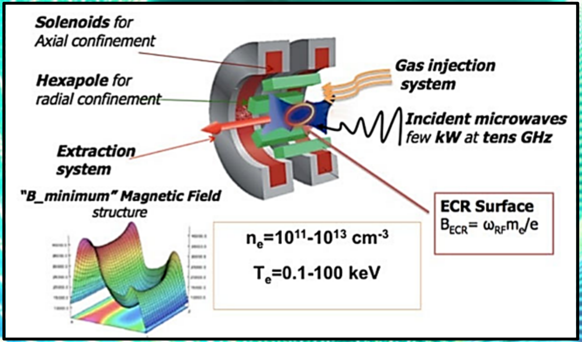

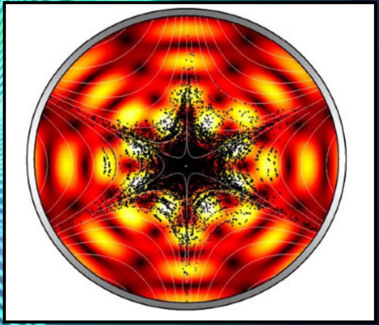

Electromagnetic field pattern in the midplane for f ~14 GHz

D. Mascali, *et al.*, Eur. Phys. J. A 53, 145 (2017).

S. Gammino, *et al.*, IEEE transactions on plasma science 36, 4 (2008).

ECR PLASMA ANISOTROPICITY

- Wave-to-particle coupling: heating process via electron cyclotron resonance (ECR)
  - RF guided wave + **multimodal structure**: highly **inhomogeneous**, **space-dependent electric field**

- **Space-dependent** and **highly-inhomogenous magnetic field** profile: plasma trapping + electron gyration

- **RESULTS: closed ECR surface for wave-particle coupling and heating**
- **RESULTS : space-dependent power transfer depending on electric field profile**

$$\omega = \omega_c = \frac{eB(r)}{m}$$

$$P \propto E(r)^2$$

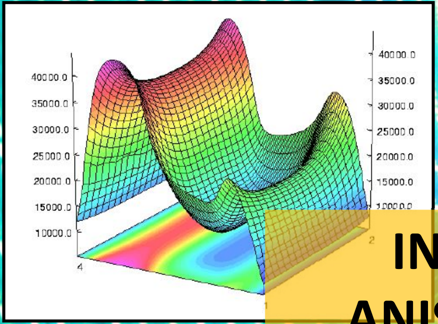

B-field profile as superposition of min-B and hexapole structures

D. Mascali, *et al.*, Eur. Phys. J. A 53, 145 (2017).

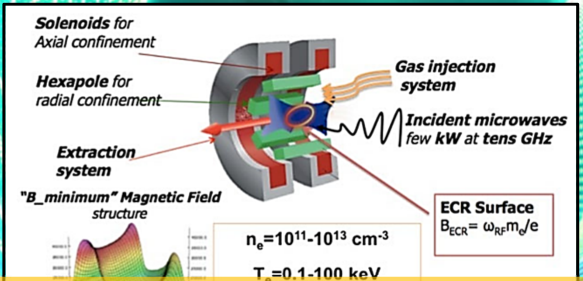

S. Gammino, *et al.*, IEEE transactions on plasma science 36, 4 (2008).

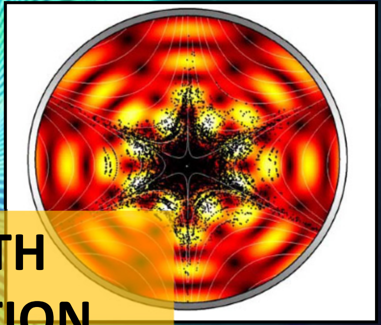

Electromagnetic field pattern in the midplane for f ~14 GHz

INHOMOGENEOUS SYSTEM WITH ANISOTROPIC ENERGY DISTRIBUTION

3D MODELING OF ELECTRON KINETICS

Istituto Nazionale di Fisica Nucleare
Laboratori Nazionali del Sud

Approach to self-consistency: 3D particle mover + 3D FEM Electromagnetic solver (INFN-LNL + INFN-LNS code)

The **EM field** distribution and the **plasma medium** influence each other in a closed loop:

3D MODELING OF ELECTRON KINETICS

INFN LNS
Istituto Nazionale di Fisica Nucleare
Laboratori Nazionali del Sud

Approach to self-consistency: 3D particle mover + 3D FEM Electromagnetic solver (INFN-LNL + INFN-LNS code)

The **EM field** distribution and the **plasma medium** influence each other in a closed loop:

EM field calculated for the empty chamber → **Tracking electrons uniformely distributed inside the chamber** → **Density map**

3D MODELING OF ELECTRON KINETICS

Approach to self-consistency: 3D particle mover + 3D FEM Electromagnetic solver (INFN-LNL + INFN-LNS code)

The **EM field** distribution and the **plasma medium** influence each other in a closed loop:

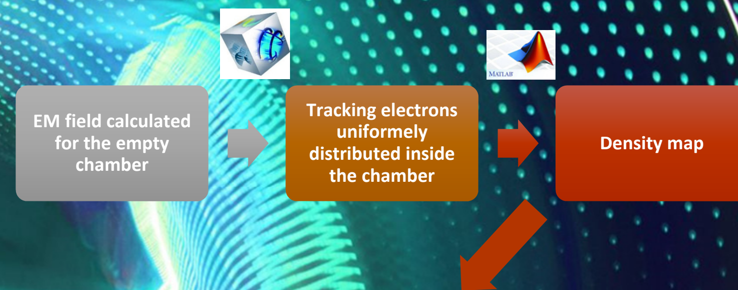

3D MODELING OF ELECTRON KINETICS

Approach to self-consistency: 3D particle mover + 3D FEM Electromagnetic solver (INFN-LNL + INFN-LNS code)

The **EM field** distribution and the **plasma medium** influence each other in a closed loop:

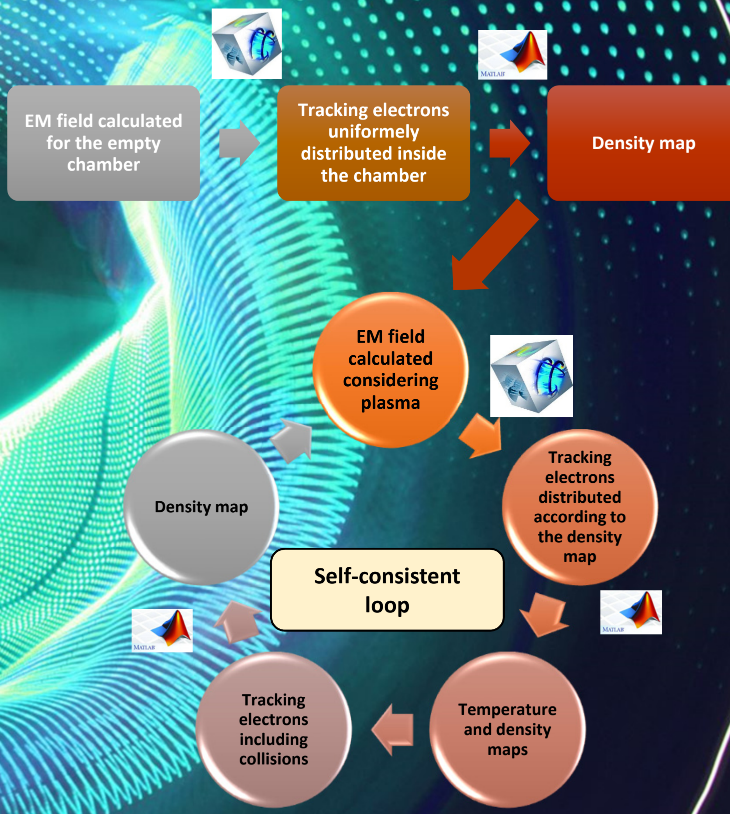

D. Mascali, Eur. Phys. J. D (2015) 69: 27

3D MODELING OF ELECTRON KINETICS

Approach to self-consistency: 3D particle mover + 3D FEM Electromagnetic solver (INFN-LNL + INFN-LNS code)

The **EM field** distribution and the **plasma medium** influence each other in a closed loop:

- Plasma concentrates in near resonance region: **dense plasmoid** egg surrounded by **rarefied halo**
- **Resonant cavity** and **mode structures** modify plasma density distribution
- **Electrons at different energies** distribute differently in the space: *cold* in the core, *hot* close to ECR boundaries

(1)

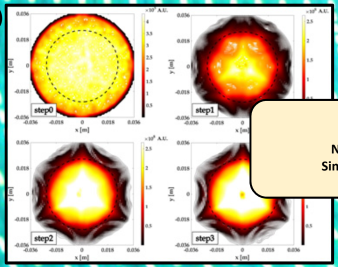

f = 14.521 GHz
Power = 100 W
N electrons = 40000
Simulation time = 40μs
Time step = 1ps

(2)

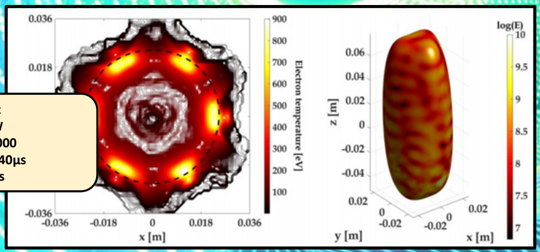

(1) z-axis projection of density maps during the calculation steps (ECR zone black dotted). (2-Left) Distribution of electron temperature in the midplane. (2-Right) Distribution of the EM field on the resonance surface.

A. Galatà, *et al.*, arXiv:1912.01988

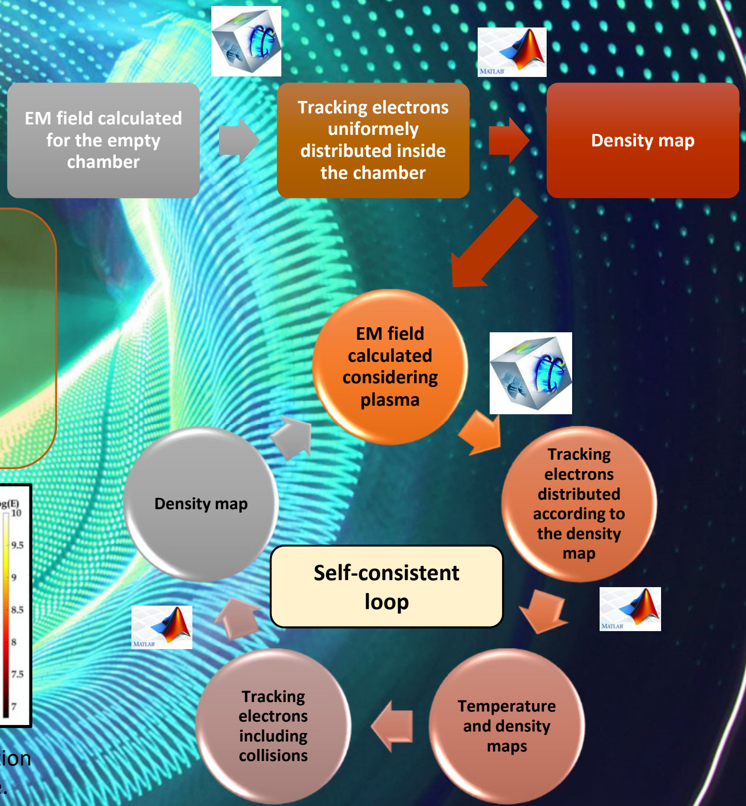

D. Mascali, Eur. Phys. J. D (2015) 69: 27

VELOCITY-SPACE ANISOTROPY DISTRIBUTION $v_\perp / v_\parallel$

INFN LNS
Istituto Nazionale di Fisica Nucleare
Laboratori Nazionali del Sud

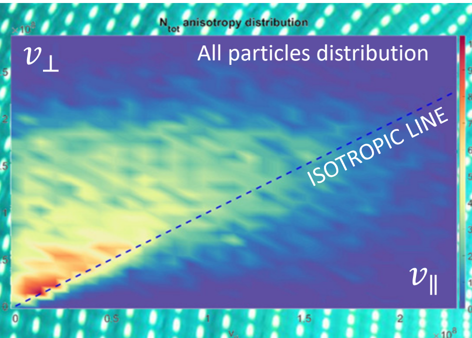

particles in chamber after t=250 µs ~ 15k
B_{min}/B_{ECR} = 0.87
f = 12.84 GHz
RF power = 400 W

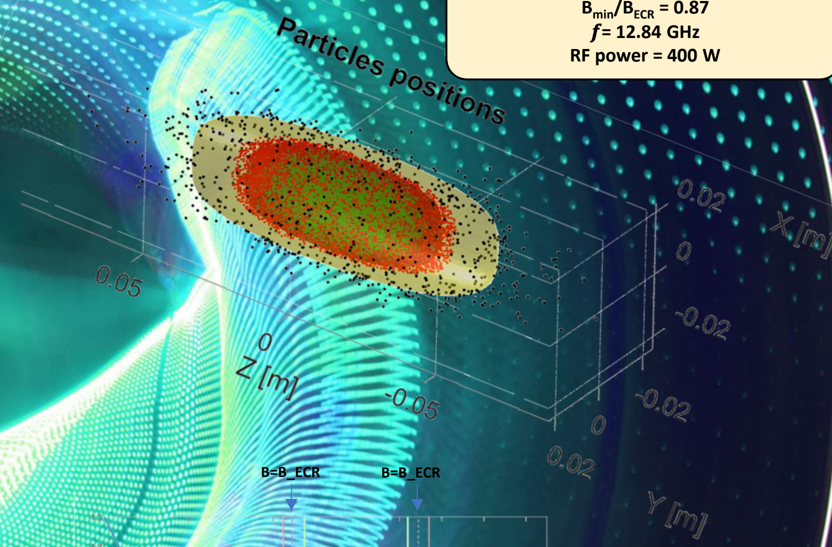

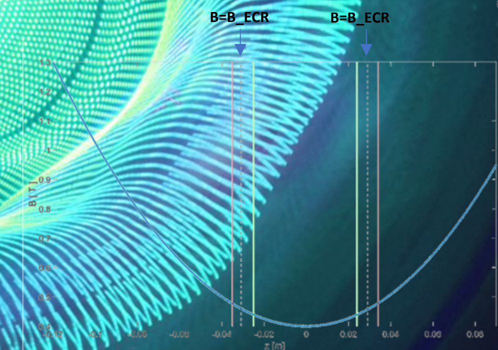

B field – profile along z-axis

- **3 collective regions** selected in the simulation domain: **(1) plasmoid egg, (2) ECR zone, (3) halo**
- **Different spread of $v_\perp$ and $v_\parallel$ -> spatial dependency**

VELOCITY-SPACE ANISOTROPY DISTRIBUTION $v_\perp / v_\parallel$

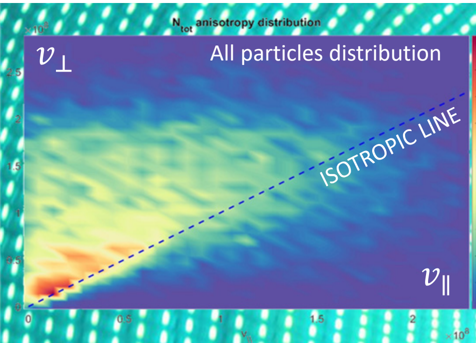

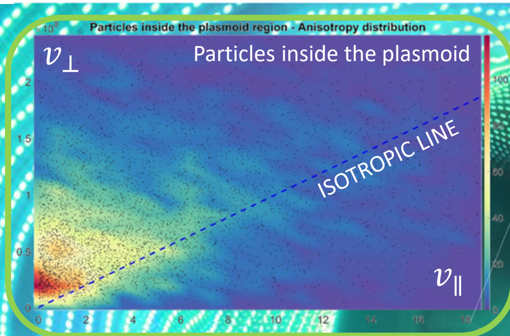

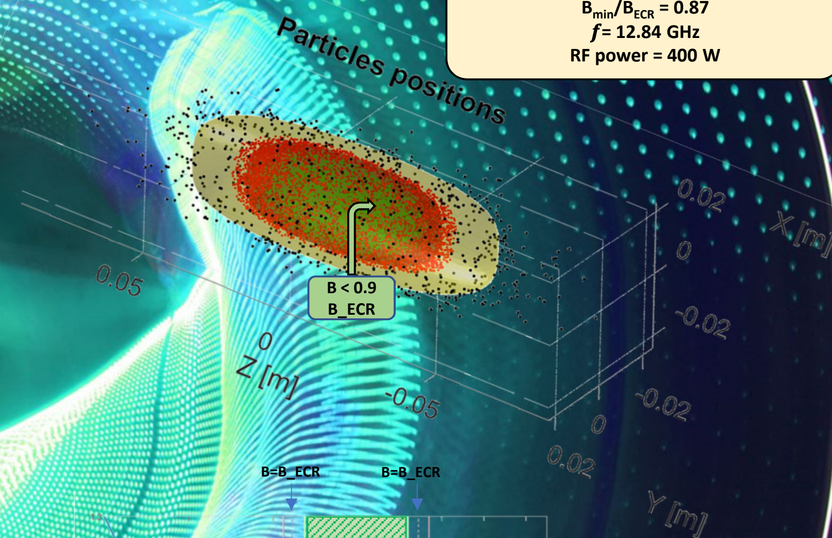

particles in chamber after t=250 µs ~ 15k
$B_{min}/B_{ECR} = 0.87$
f= 12.84 GHz
RF power = 400 W

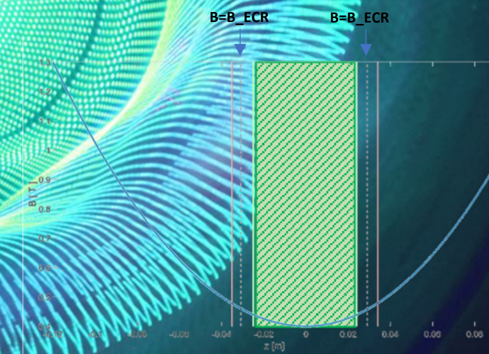

B field – profile along z-axis

- **3 collective regions** selected in the simulation domain: **(1) plasmoid egg, (2) ECR zone, (3) halo**
- **Different spread of $v_\perp$ and $v_\parallel$ -> spatial dependency**

VELOCITY-SPACE ANISOTROPY DISTRIBUTION $v_\perp / v_\parallel$

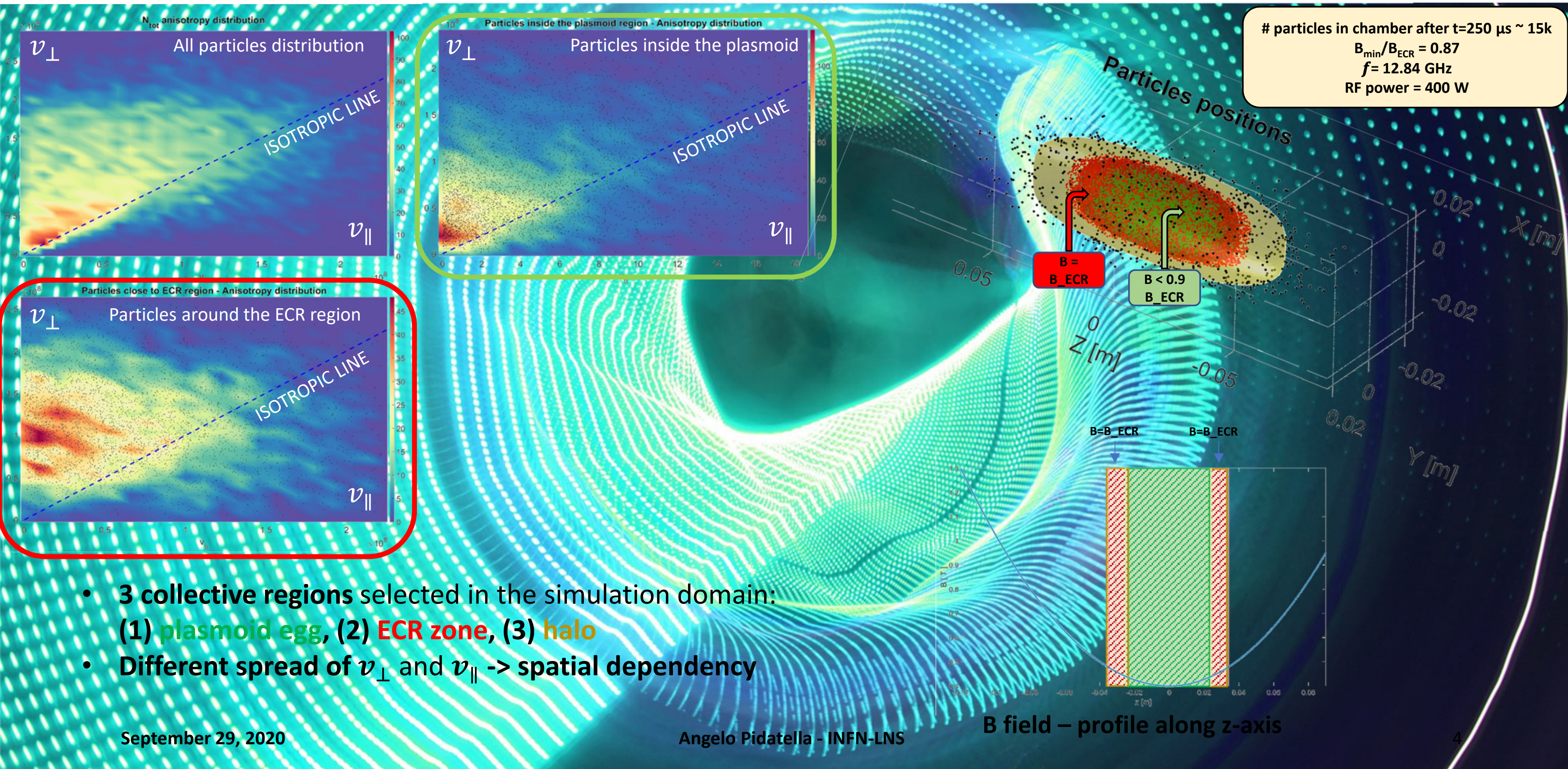

- **3 collective regions** selected in the simulation domain: **(1) plasmoid egg, (2) ECR zone, (3) halo**
- **Different spread of $v_\perp$ and $v_\parallel$ -> spatial dependency**

B field – profile along z-axis

VELOCITY-SPACE ANISOTROPY DISTRIBUTION $v_\perp / v_\parallel$

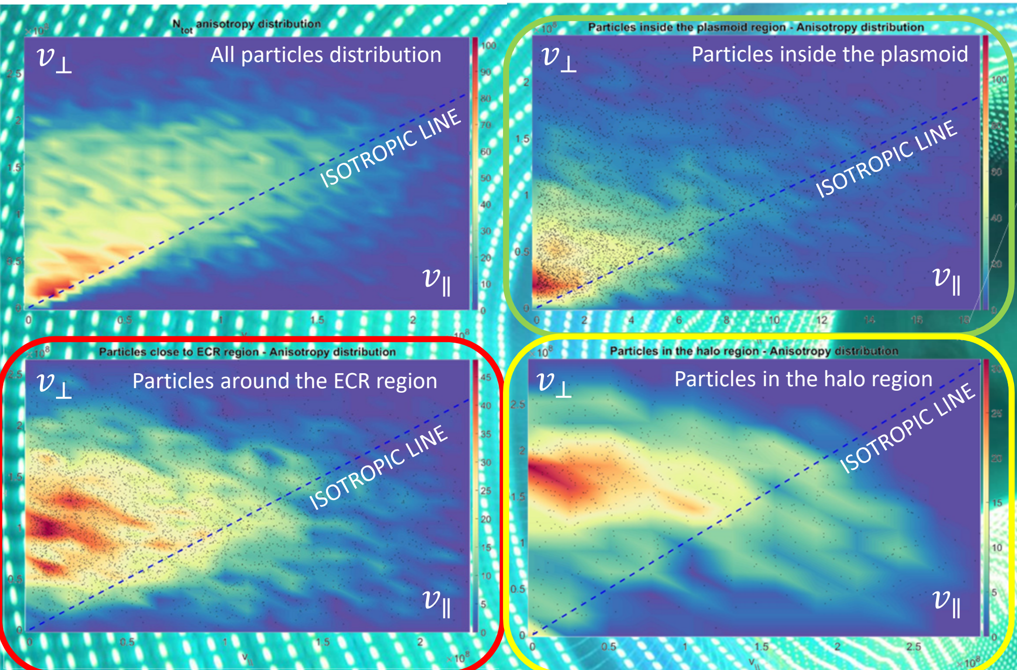

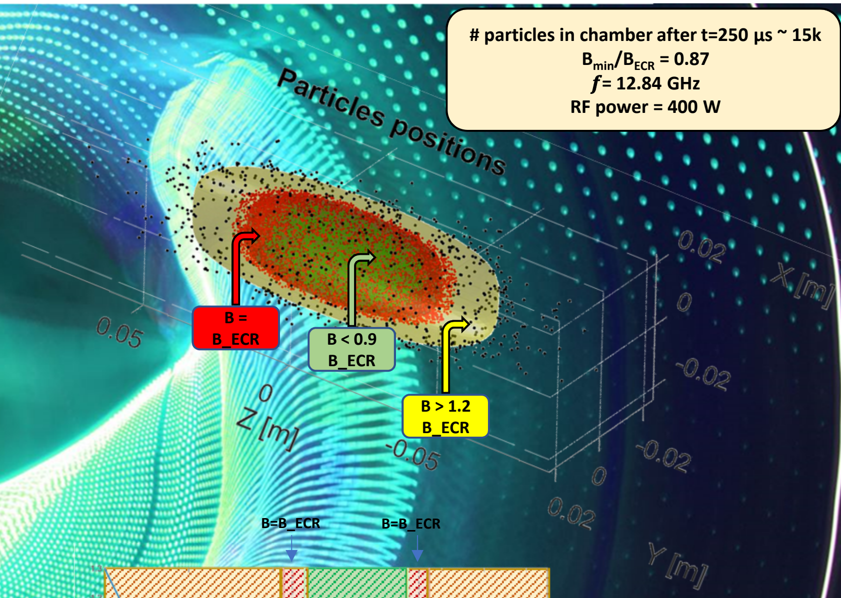

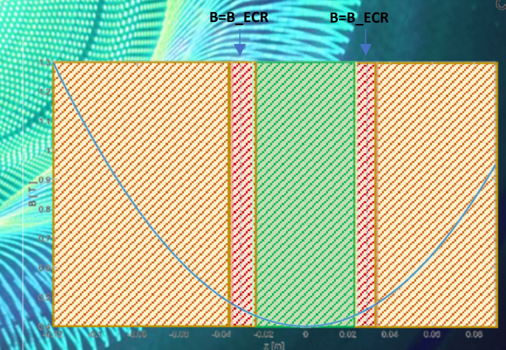

B field – profile along z-axis

- **3 collective regions** selected in the simulation domain: **(1) plasmoid egg, (2) ECR zone, (3) halo**
- **Different spread of $v_\perp$ and $v_\parallel$ -> spatial dependency**

VELOCITY-SPACE ANISOTROPY DISTRIBUTION $v_\perp / v_\parallel$

INFN LNS
Istituto Nazionale di Fisica Nucleare
Laboratori Nazionali del Sud

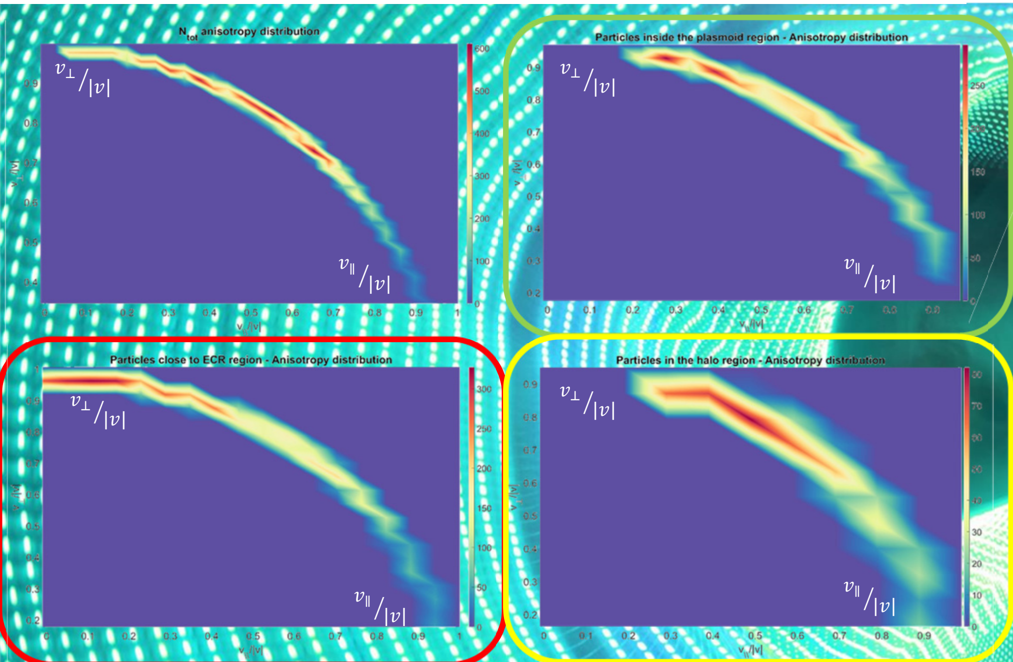

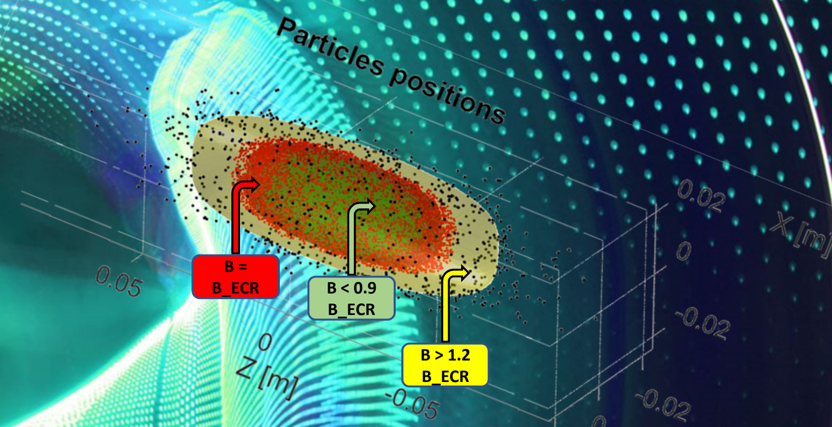

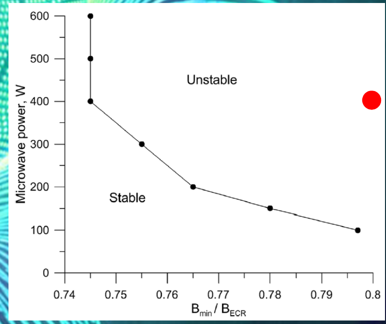

V. Skalyga, *et al.*, Physics of Plasma 22, 083509 (2015)

● $B_{min}/B_{ECR} = 0.87$
Power = 400 W

While inside the plasmoid egg, particles show **prominent isotropic distribution** (few particles with $v_\perp / v_\parallel \sim \mathbf{2 \div 4}$), the ECR region show **many anisotropic particles** with $v_\perp / v_\parallel \geq \mathbf{10}$

VELOCITY-SPACE ANISOTROPY DISTRIBUTION $v_\perp / v_\parallel$

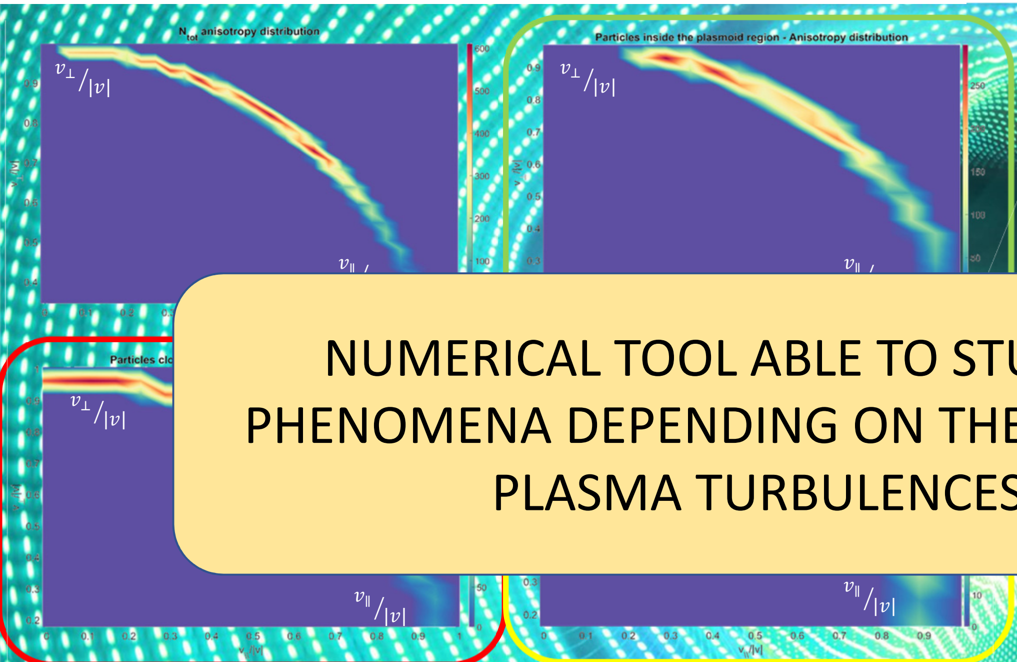

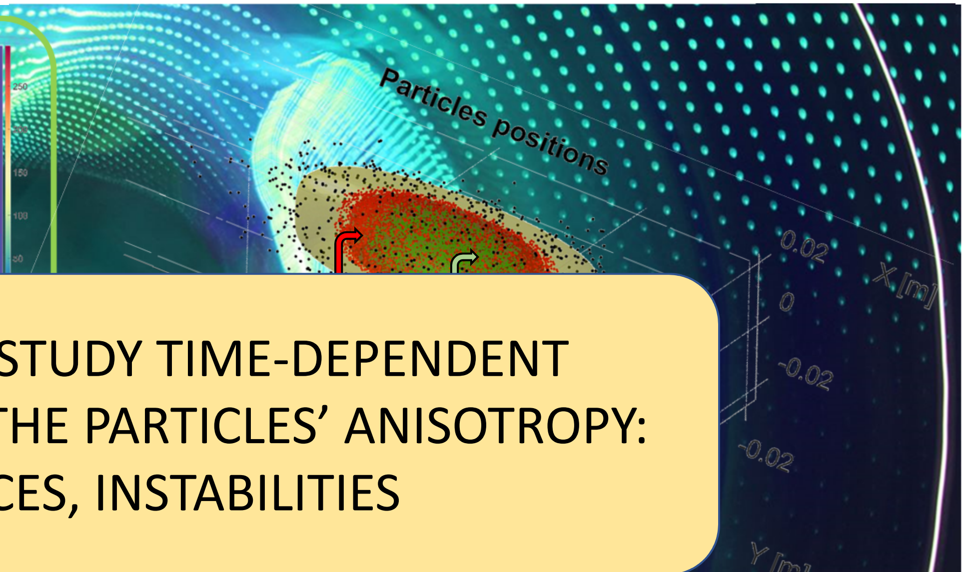

NUMERICAL TOOL ABLE TO STUDY TIME-DEPENDENT PHENOMENA DEPENDING ON THE PARTICLES' ANISOTROPY: PLASMA TURBULENCES, INSTABILITIES

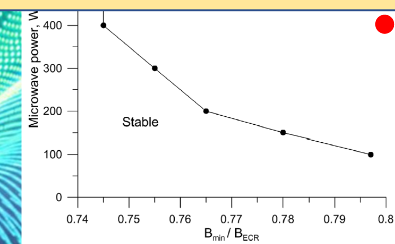

V. Skalyga, *et al.*, Physics of Plasma 22, 083509 (2015)

$B_{min}/B_{ECR} = 0.87$
Power = 400 W

While inside the plasmoid egg, particles show **prominent isotropic distribution** (few particles with $v_\perp/v_\parallel \sim \mathbf{2 \div 4}$), the ECR region show **many anisotropic particles** with $v_\perp/v_\parallel \geq \mathbf{10}$

ECR REGION ANISOTROPY DISTRIBUTION $v_{\perp}/v_{\parallel}$

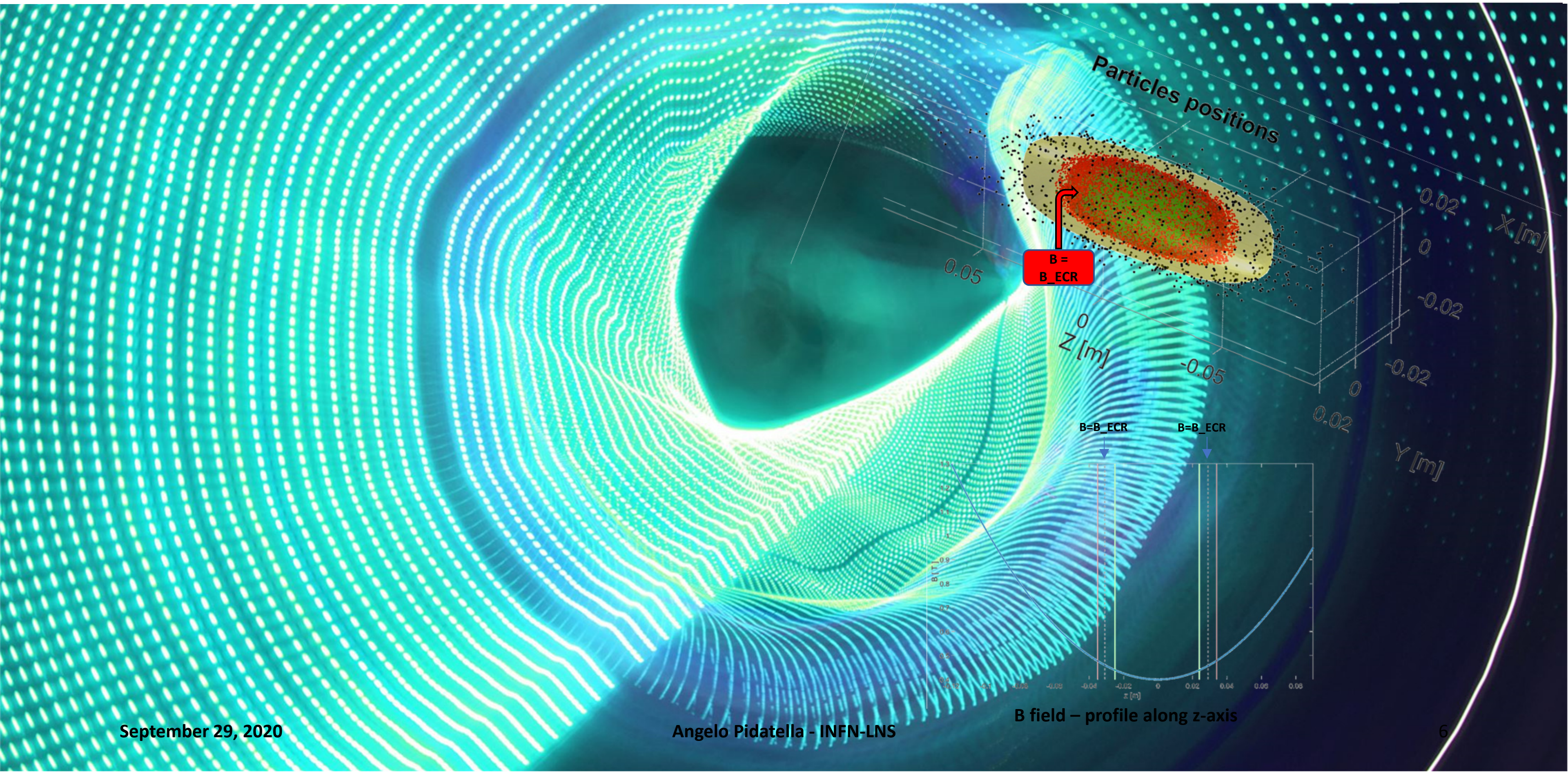

ECR REGION ANISOTROPY DISTRIBUTION $v_\perp / v_\parallel$

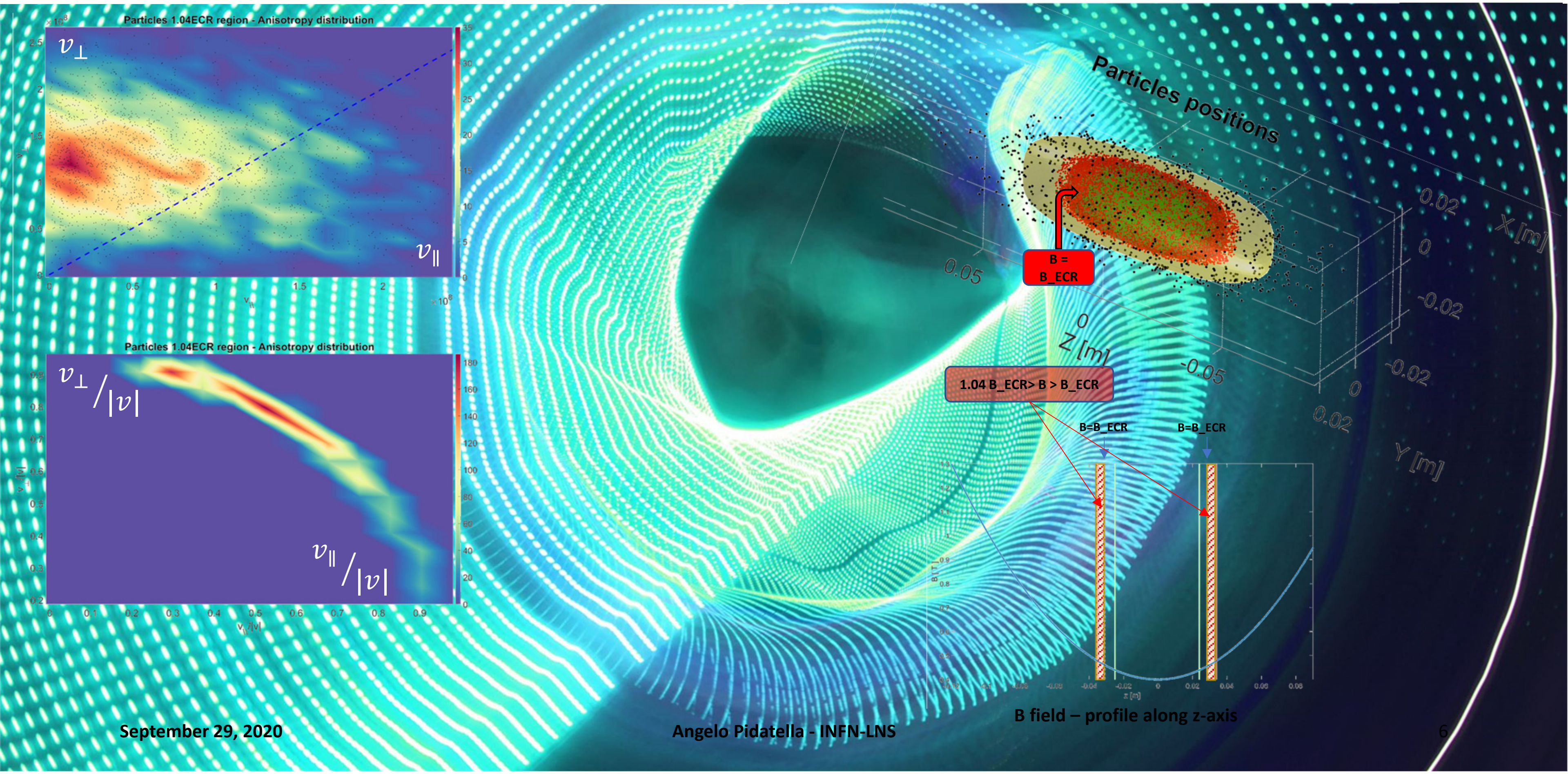

ECR REGION ANISOTROPY DISTRIBUTION $v_\perp / v_\parallel$

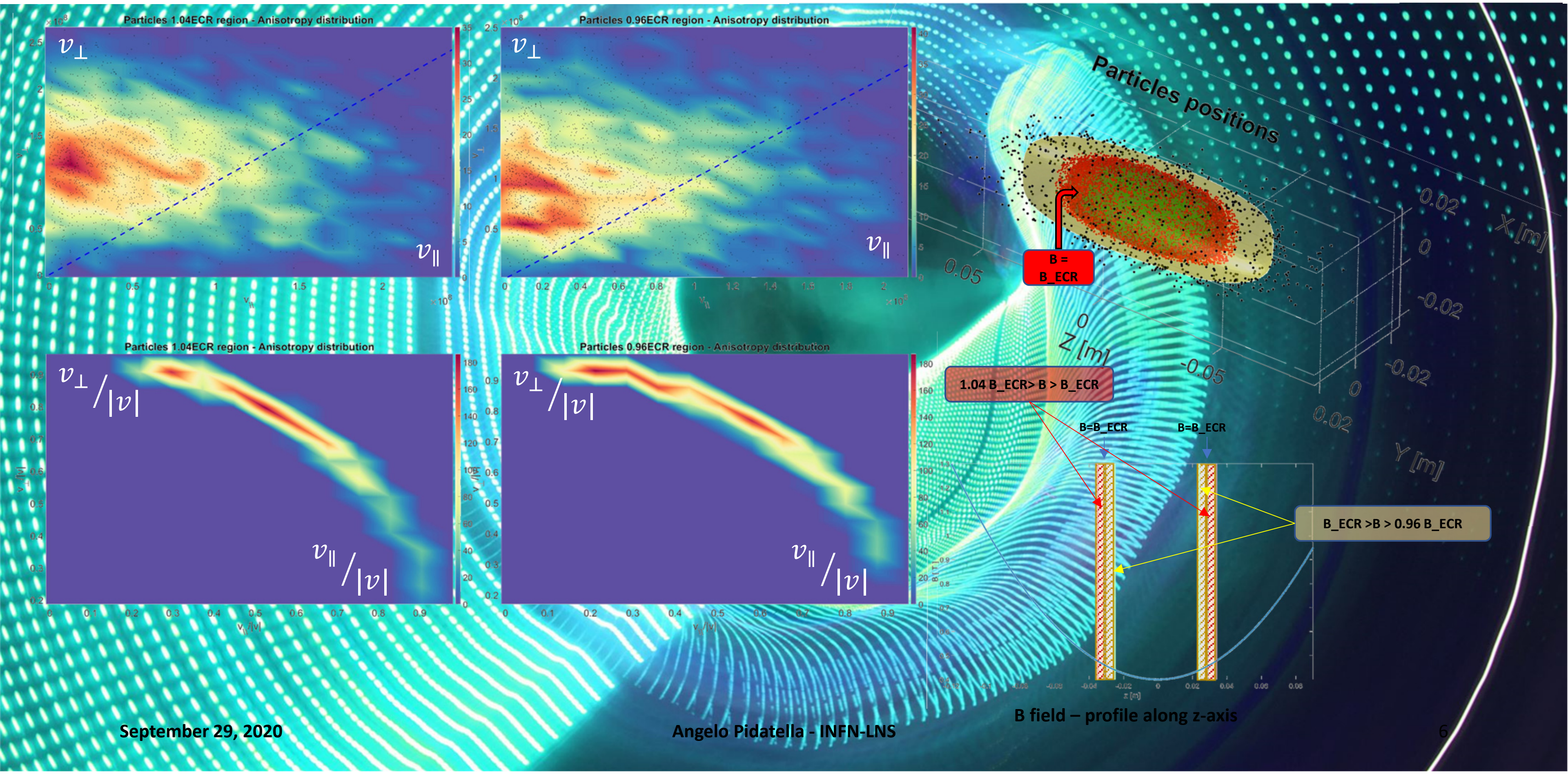

ECR REGION ANISOTROPY DISTRIBUTION $v_{\perp}/v_{\parallel}$

Istituto Nazionale di Fisica Nucleare
Laboratori Nazionali del Sud

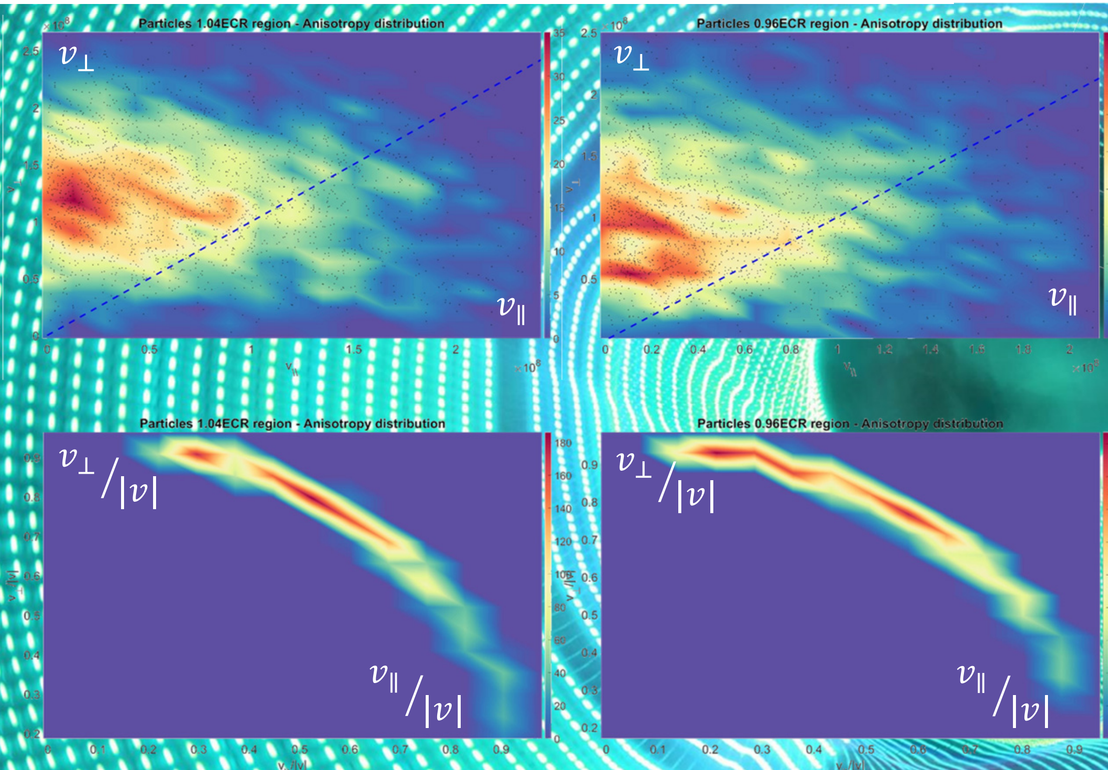

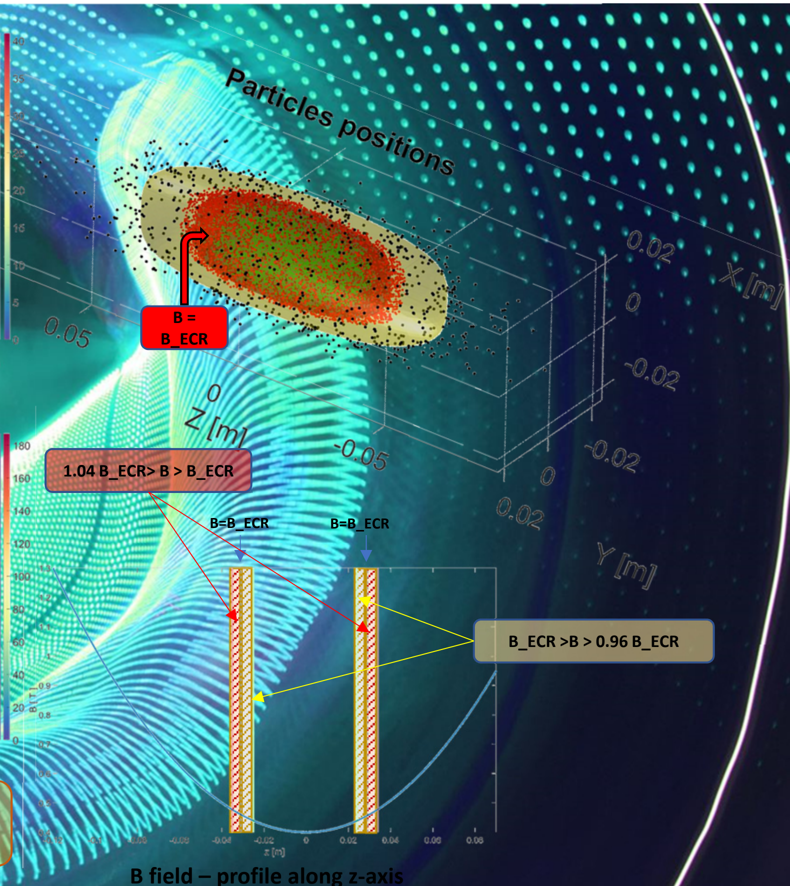

Around the **ECR isosurface: inner** particles slightly **more anisotropic** than the **outer ones**

ECR REGION ANISOTROPY DISTRIBUTION $v_{\perp}/v_{\parallel}$

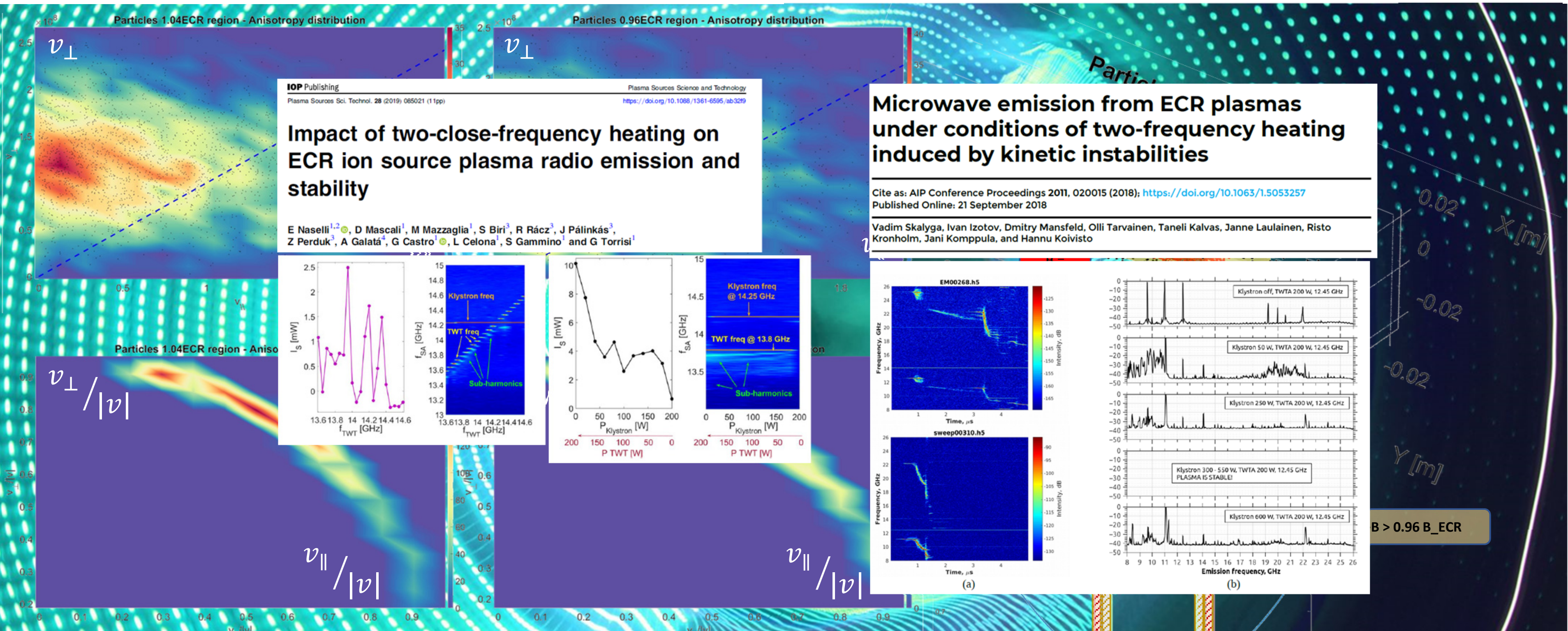

IOP Publishing
Plasma Sources Science and Technology
Plasma Sources Sci. Technol. 28 (2019) 085021 (11pp)
https://doi.org/10.1088/1361-6595/ab32f9

Impact of two-close-frequency heating on ECR ion source plasma radio emission and stability

E Naselli[1,2], D Mascali[1], M Mazzaglia[1], S Biri[3], R Rácz[3], J Pálinkás[3], Z Perduk[3], A Galatá[4], G Castro[1], L Celona[1], S Gammino[1] and G Torrisi[1]

Microwave emission from ECR plasmas under conditions of two-frequency heating induced by kinetic instabilities

Cite as: AIP Conference Proceedings 2011, 020015 (2018); https://doi.org/10.1063/1.5053257
Published Online: 21 September 2018

Vadim Skalyga, Ivan Izotov, Dmitry Mansfeld, Olli Tarvainen, Taneli Kalvas, Janne Laulainen, Risto Kronholm, Jani Komppula, and Hannu Koivisto

B field – profile along z-axis

Around the **ECR isosurface: inner** particles slightly **more anisotropic** than the **outer ones**

SPACE-RESOLVED ELECTRON ENERGY DISTRIBUTION FUNCTION (EEDF)

(Submission paper in progress)

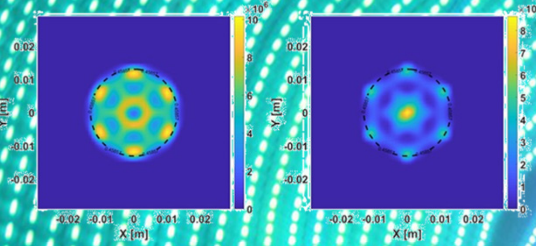

XY-projections of electron occupation maps in 2-4 (left) and 6-8 keV (right), and ECR surface contour

Simulation data:
f= 12.84 GHz
RF power = 30 W

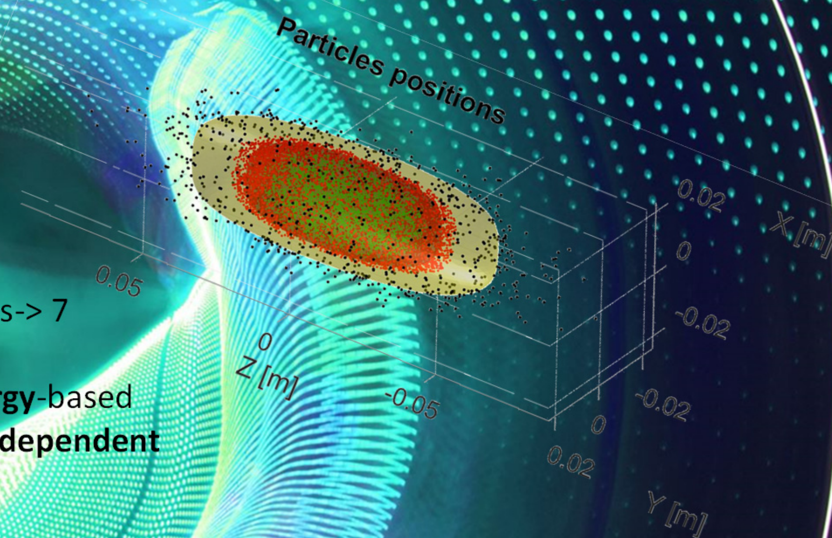

1° Step: division of plasma regions in electron energy intervals-> 7 intervals [0-2], [2-4] … [12-∞] keV

2° Step: separate plasma into different electron **average-energy**-based **regions of interest** (**ROI**s), **assuming** each ROI as containing **independent electron populations.**

SPACE-RESOLVED ELECTRON ENERGY DISTRIBUTION FUNCTION (EEDF)

(Submission paper in progress)

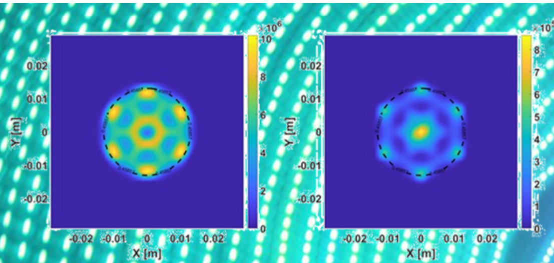

XY-projections of electron occupation maps in 2-4 (left) and 6-8 keV (right), and ECR surface contour

Simulation data:
f = 12.84 GHz
RF power = 30 W

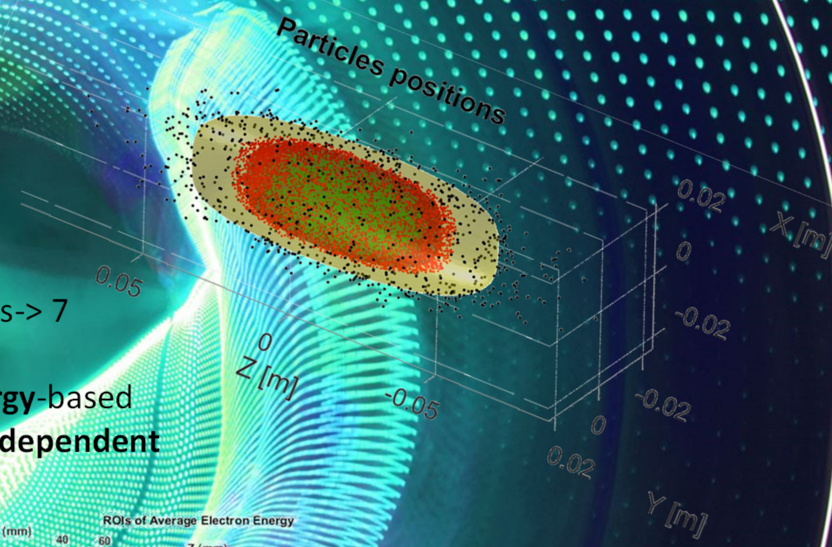

1° Step: division of plasma regions in electron energy intervals-> 7 intervals [0-2], [2-4] … [12-∞] keV

2° Step: separate plasma into different electron **average-energy**-based **regions of interest** (**ROI**s), **assuming** each ROI as containing **independent electron populations.**

AVERAGE ELECTRON ENERGY $\langle E \rangle = \frac{\sum_{i=1}^{7} \rho_i E_i}{\sum_{i=1}^{7} \rho_i}$

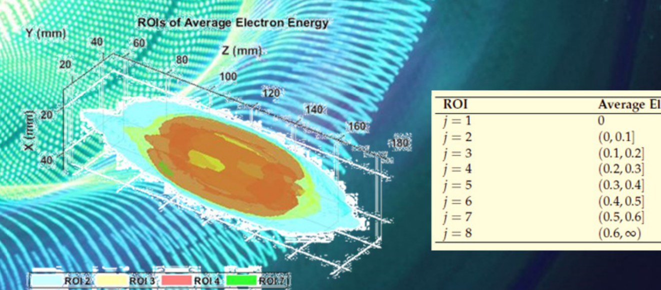

ROI	Average Electron Energy(keV)
$j = 1$	0
$j = 2$	(0, 0.1]
$j = 3$	(0.1, 0.2]
$j = 4$	(0.2, 0.3]
$j = 5$	(0.3, 0.4]
$j = 6$	(0.4, 0.5]
$j = 7$	(0.5, 0.6]
$j = 8$	(0.6, ∞)

SPACE-RESOLVED ELECTRON ENERGY DISTRIBUTION FUNCTION (EEDF)

(Submission paper in progress)

Simulation data:
f = 12.84 GHz
RF power = 30 W

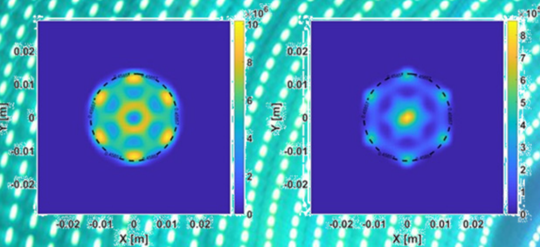

XY-projections of electron occupation maps in 2-4 (left) and 6-8 keV (right), and ECR surface contour

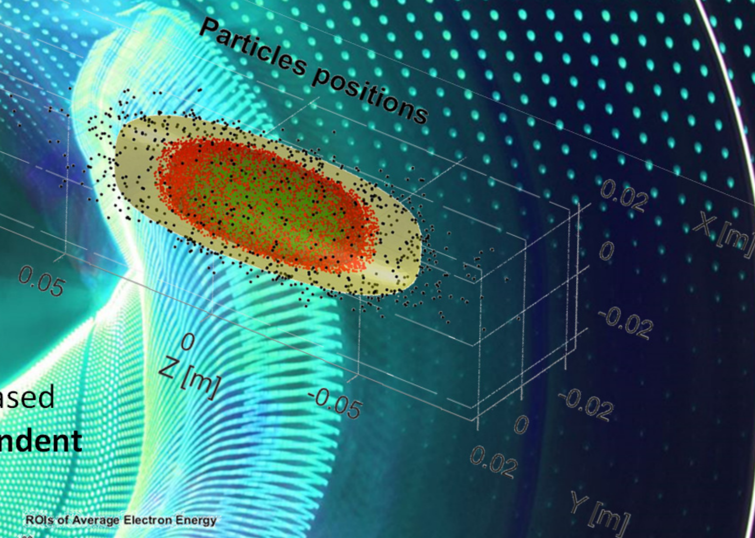

1° Step: division of plasma regions in electron energy intervals-> 7 intervals [0-2], [2-4] … [12-∞] keV

2° Step: separate plasma into different electron **average-energy**-based **regions of interest** (**ROI**s), **assuming** each ROI as containing **independent electron populations.**

AVERAGE ELECTRON ENERGY $\langle E \rangle = \frac{\sum_{i=1}^{7} \rho_i E_i}{\sum_{i=1}^{7} \rho_i}$

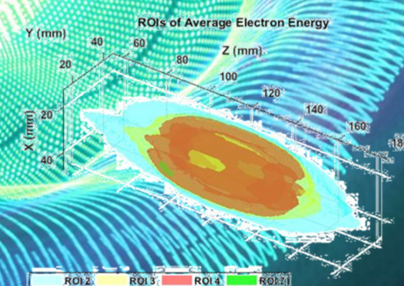

ROI	Average Electron Energy(keV)
$j = 1$	0
$j = 2$	(0, 0.1]
$j = 3$	(0.1, 0.2]
$j = 4$	(0.2, 0.3]
$j = 5$	(0.3, 0.4]
$j = 6$	(0.4, 0.5]
$j = 7$	(0.5, 0.6]
$j = 8$	(0.6, ∞)

GOAL: study the nature of local EEDF in each of these ROIs; continuous EEDF from discrete electron data.

SPACE-RESOLVED ELECTRON ENERGY DISTRIBUTION FUNCTION (EEDF)

(Submission paper in progress)

INFN LNS
Istituto Nazionale di Fisica Nucleare
Laboratori Nazionali del Sud

2-components test EEDFs: capturing low-T and high-T properties (**EEDF1** and **EEDF2**)
3-components test EEDFs: low-T + mid-T + high-T properties (**EEDF3** and **EEDF 4**)

Ref. case name	**Type**
EEDF1	Low-E f_M + High-E f_M
EEDF2	Low-E f_M + High-E f_D
EEDF3	Low-E f_M + Medium-E f_M + High-E f_M
EEDF4	Low-E f_M + Medium-E f_D + High-E f_M

SPACE-RESOLVED ELECTRON ENERGY DISTRIBUTION FUNCTION (EEDF)

(Submission paper in progress)

Istituto Nazionale di Fisica Nucleare
Laboratori Nazionali del Sud

2-components test EEDFs: capturing low-T and high-T properties (**EEDF1** and **EEDF2**)

3-components test EEDFs: low-T + mid-T + high-T properties (**EEDF3** and **EEDF 4**)

Ref. case name	Type
EEDF1	Low-E f_M + High-E f_M
EEDF2	Low-E f_M + High-E f_D
EEDF3	Low-E f_M + Medium-E f_M + High-E f_M
EEDF4	Low-E f_M + Medium-E f_D + High-E f_M

BEST EEDF2: LOW-MAXWELLIAN + HIGH-DRUYVESTEYN

$$f(E,kT_1,kT_2) = N_1\left(\frac{2}{\sqrt{\pi}}\frac{\sqrt{E}}{\sqrt{(kT_1)^3}}e^{-E/kT_1}\right) + N_2\left(1.04\frac{\sqrt{E}}{\sqrt{(kT_2)^3}}e^{-0.55E^2/(kT_2)^2}\right)$$

SPACE-RESOLVED ELECTRON ENERGY DISTRIBUTION FUNCTION (EEDF)

(Submission paper in progress)

Istituto Nazionale di Fisica Nucleare
Laboratori Nazionali del Sud

2-components test EEDFs: capturing low-T and high-T properties (**EEDF1** and **EEDF2**)

3-components test EEDFs: low-T + mid-T + high-T properties (**EEDF3** and **EEDF 4**)

Ref. case name	Type
EEDF1	Low-E f_M + High-E f_M
EEDF2	Low-E f_M + High-E f_D
EEDF3	Low-E f_M + Medium-E f_M + High-E f_M
EEDF4	Low-E f_M + Medium-E f_D + High-E f_M

BEST EEDF2: LOW-MAXWELLIAN + HIGH-DRUYVESTEYN

$$f(E, kT_1, kT_2) = N_1\left(\frac{2}{\sqrt{\pi}}\frac{\sqrt{E}}{\sqrt{(kT_1)^3}}e^{-E/kT_1}\right) + N_2\left(1.04\frac{\sqrt{E}}{\sqrt{(kT_2)^3}}e^{-0.55E^2/(kT_2)^2}\right)$$

Fit parameters

$$(\mathrm{k_B T}_l)_j = \frac{2}{3}\mathrm{C}_j\mathrm{E}_{1j}, \quad (\mathrm{k_B T}_h)_j = \mathrm{S}_j\frac{\sum_{i=2}^{7}\rho_{ij}\mathrm{E}_{ij}}{\sum_{i=2}^{7}\rho_{ij}}$$

Fit analysis

$$\langle MSE\rangle_j = \frac{1}{N(j)}\sum_{k(j)=1}^{N(j)} MSE_{k(j)},$$

$$\sigma_{\langle MSE\rangle_j} = \frac{1}{\sqrt{N(j)-1}}\sqrt{\sum_{k(j)=1}^{N(j)}(MSE_{k(j)} - \langle MSE\rangle_j)^2}$$

$$\langle r^2\rangle_j = \frac{1}{N(j)}\sum_{k(j)=1}^{N(j)}(r^2)_{k(j)},$$

$$\sigma_{\langle r^2\rangle_j} = \frac{1}{\sqrt{N(j)-1}}\sqrt{\sum_{k(j)=1}^{N(j)}((r^2)_{k(j)} - \langle r^2\rangle_j)^2}$$

<u>SPACE-RESOLVED</u> ELECTRON ENERGY DISTRIBUTION FUNCTION (EEDF)

(Submission paper in progress)

2-components test EEDFs: capturing low-T and high-T properties (**EEDF1** and **EEDF2**)

3-components test EEDFs: low-T + mid-T + high-T properties (**EEDF3** and **EEDF 4**)

Ref. case name	Type
EEDF1	Low-E f_M + High-E f_M
EEDF2	Low-E f_M + High-E f_D
EEDF3	Low-E f_M + Medium-E f_M + High-E f_M
EEDF4	Low-E f_M + Medium-E f_D + High-E f_M

BEST EEDF2: LOW-MAXWELLIAN + HIGH-DRUYVESTEYN

$$f(E,kT_1,kT_2) = N_1\left(\frac{2}{\sqrt{\pi}}\frac{\sqrt{E}}{\sqrt{(kT_1)^3}}e^{-E/kT_1}\right) + N_2\left(1.04\frac{\sqrt{E}}{\sqrt{(kT_2)^3}}e^{-0.55E^2/(kT_2)^2}\right)$$

Qualitative analysis on j-th ROI-aggregated collective data for the i-th energy interval

Fit parameters

$$(\mathrm{k_B T}_l)_j = \frac{2}{3}\mathrm{C}_j\mathrm{E}_{1j}, \quad (\mathrm{k_B T}_h)_j = \mathrm{S}_j\frac{\sum_{i=2}^{7}\rho_{ij}\mathrm{E}_{ij}}{\sum_{i=2}^{7}\rho_{ij}}$$

Fit analysis

$$\langle MSE\rangle_j = \frac{1}{N(j)}\sum_{k(j)=1}^{N(j)} MSE_{k(j)},$$

$$\sigma_{\langle MSE\rangle_j} = \frac{1}{\sqrt{N(j)-1}}\sqrt{\sum_{k(j)=1}^{N(j)}(MSE_{k(j)} - \langle MSE\rangle_j)^2}$$

$$\langle r^2\rangle_j = \frac{1}{N(j)}\sum_{k(j)=1}^{N(j)}(r^2)_{k(j)},$$

$$\sigma_{\langle r^2\rangle_j} = \frac{1}{\sqrt{N(j)-1}}\sqrt{\sum_{k(j)=1}^{N(j)}((r^2)_{k(j)} - \langle r^2\rangle_j)^2}$$

<u>SPACE-RESOLVED</u> ELECTRON ENERGY DISTRIBUTION FUNCTION (EEDF)

(Submission paper in progress)

2-components test EEDFs: capturing low-T and high-T properties (**EEDF1** and **EEDF2**)

3-components test EEDFs: low-T + mid-T + high-T properties (**EEDF3** and **EEDF 4**)

Ref. case name	Type
EEDF1	Low-E f_M + High-E f_M
EEDF2	Low-E f_M + High-E f_D
EEDF3	Low-E f_M + Medium-E f_M + High-E f_M
EEDF4	Low-E f_M + Medium-E f_D + High-E f_M

BEST EEDF2: LOW-MAXWELLIAN + HIGH-DRUYVESTEYN

$$f(E, kT_1, kT_2) = N_1\left(\frac{2}{\sqrt{\pi}}\frac{\sqrt{E}}{\sqrt{(kT_1)^3}}e^{-E/kT_1}\right) + N_2\left(1.04\frac{\sqrt{E}}{\sqrt{(kT_2)^3}}e^{-0.55E^2/(kT_2)^2}\right)$$

Qualitative analysis on j-th ROI-aggregated collective data for the i-th energy interval

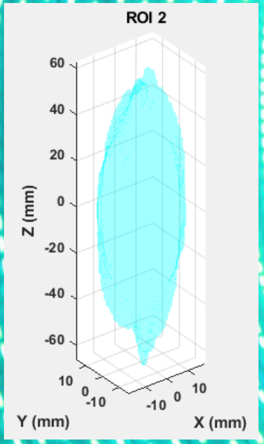

Fit parameters

$$(k_B T_l)_j = \frac{2}{3}C_j E_{1j}, \quad (k_B T_h)_j = S_j \frac{\sum_{i=2}^{7} \rho_{ij} E_{ij}}{\sum_{i=2}^{7} \rho_{ij}}$$

Fit analysis

$$\langle MSE \rangle_j = \frac{1}{N(j)} \sum_{k(j)=1}^{N(j)} MSE_{k(j)},$$

$$\sigma_{\langle MSE \rangle_j} = \frac{1}{\sqrt{N(j)-1}} \sqrt{\sum_{k(j)=1}^{N(j)} (MSE_{k(j)} - \langle MSE \rangle_j)^2}$$

$$\langle r^2 \rangle_j = \frac{1}{N(j)} \sum_{k(j)=1}^{N(j)} (r^2)_{k(j)},$$

$$\sigma_{\langle r^2 \rangle_j} = \frac{1}{\sqrt{N(j)-1}} \sqrt{\sum_{k(j)=1}^{N(j)} ((r^2)_{k(j)} - \langle r^2 \rangle_j)^2}$$

SPACE-RESOLVED ELECTRON ENERGY DISTRIBUTION FUNCTION (EEDF)

(Submission paper in progress)

2-components test EEDFs: capturing low-T and high-T properties (**EEDF1** and **EEDF2**)
3-components test EEDFs: low-T + mid-T + high-T properties (**EEDF3** and **EEDF 4**)

Ref. case name	Type
EEDF1	Low-E f_M + High-E f_M
EEDF2	Low-E f_M + High-E f_D
EEDF3	Low-E f_M + Medium-E f_M + High-E f_M
EEDF4	Low-E f_M + Medium-E f_D + High-E f_M

BEST EEDF2: LOW-MAXWELLIAN + HIGH-DRUYVESTEYN

$$f(E,kT_1,kT_2) = N_1\left(\frac{2}{\sqrt{\pi}}\frac{\sqrt{E}}{\sqrt{(kT_1)^3}}e^{-E/kT_1}\right) + N_2\left(1.04\frac{\sqrt{E}}{\sqrt{(kT_2)^3}}e^{-0.55E^2/(kT_2)^2}\right)$$

Qualitative analysis on j-th ROI-aggregated collective data for the i-th energy interval

$$(\boldsymbol{\rho}_{ij})_{est} = (\sum_{i=1}^{7}\boldsymbol{\rho}_{ij})\int_a^b f(E;(\mathbf{k_B T}_l)_j;(\mathbf{k_B T}_h)_j)\mathrm{d}E$$

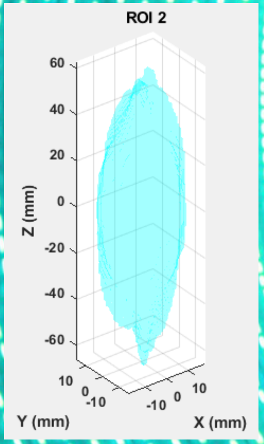

Fit parameters

$$(\mathbf{k_B T}_l)_j = \frac{2}{3}\mathbf{C}_j\mathbf{E}_{1j}, \quad (\mathbf{k_B T}_h)_j = \mathbf{S}_j\frac{\sum_{i=2}^{7}\boldsymbol{\rho}_{ij}\mathbf{E}_{ij}}{\sum_{i=2}^{7}\boldsymbol{\rho}_{ij}}$$

Fit analysis

$$\langle MSE\rangle_j = \frac{1}{N(j)}\sum_{k(j)=1}^{N(j)} MSE_{k(j)},$$

$$\sigma_{\langle MSE\rangle_j} = \frac{1}{\sqrt{N(j)-1}}\sqrt{\sum_{k(j)=1}^{N(j)}(MSE_{k(j)} - \langle MSE\rangle_j)^2}$$

$$\langle r^2\rangle_j = \frac{1}{N(j)}\sum_{k(j)=1}^{N(j)}(r^2)_{k(j)},$$

$$\sigma_{\langle r^2\rangle_j} = \frac{1}{\sqrt{N(j)-1}}\sqrt{\sum_{k(j)=1}^{N(j)}((r^2)_{k(j)} - \langle r^2\rangle_j)^2}$$

<u>SPACE-RESOLVED</u> ELECTRON ENERGY DISTRIBUTION FUNCTION (EEDF)

(Submission paper in progress)

Istituto Nazionale di Fisica Nucleare
Laboratori Nazionali del Sud

2-components test EEDFs: capturing low-T and high-T properties (**EEDF1** and **EEDF2**)

3-components test EEDFs: low-T + mid-T + high-T properties (**EEDF3** and **EEDF 4**)

Ref. case name	Type
EEDF1	Low-E f_M + High-E f_M
EEDF2	Low-E f_M + High-E f_D
EEDF3	Low-E f_M + Medium-E f_M + High-E f_M
EEDF4	Low-E f_M + Medium-E f_D + High-E f_M

BEST EEDF2: LOW-MAXWELLIAN + HIGH-DRUYVESTEYN

$$f(E, kT_1, kT_2) = N_1\left(\frac{2}{\sqrt{\pi}}\frac{\sqrt{E}}{\sqrt{(kT_1)^3}}e^{-E/kT_1}\right) + N_2\left(1.04\frac{\sqrt{E}}{\sqrt{(kT_2)^3}}e^{-0.55E^2/(kT_2)^2}\right)$$

Qualitative analysis on j-th ROI-aggregated collective data for the i-th energy interval

$$(\boldsymbol{\rho}_{ij})_{est} = \left(\sum_{i=1}^{7}\boldsymbol{\rho}_{ij}\right)\int_a^b f(E; (\mathbf{k_B T}_l)_j; (\mathbf{k_B T}_h)_j)\mathrm{d}E$$

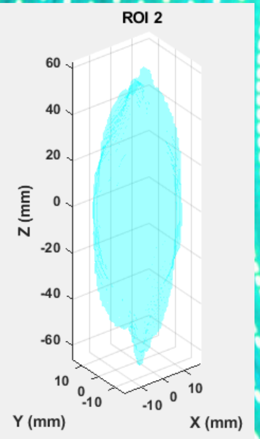

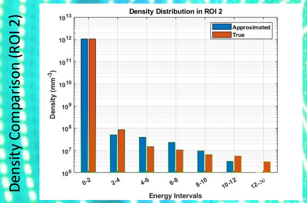

Fit parameters

$$(\mathrm{k_B T}_l)_j = \frac{2}{3}\mathrm{C}_j\mathrm{E}_{1j}, \quad (\mathrm{k_B T}_h)_j = \mathrm{S}_j\frac{\sum_{i=2}^{7}\rho_{ij}\mathrm{E}_{ij}}{\sum_{i=2}^{7}\rho_{ij}}$$

Fit analysis

$$\langle MSE\rangle_j = \frac{1}{N(j)}\sum_{k(j)=1}^{N(j)} MSE_{k(j)},$$

$$\sigma_{\langle MSE\rangle_j} = \frac{1}{\sqrt{N(j)-1}}\sqrt{\sum_{k(j)=1}^{N(j)}(MSE_{k(j)} - \langle MSE\rangle_j)^2}$$

$$\langle r^2\rangle_j = \frac{1}{N(j)}\sum_{k(j)=1}^{N(j)}(r^2)_{k(j)},$$

$$\sigma_{\langle r^2\rangle_j} = \frac{1}{\sqrt{N(j)-1}}\sqrt{\sum_{k(j)=1}^{N(j)}((r^2)_{k(j)} - \langle r^2\rangle_j)^2}$$

SPACE-RESOLVED ELECTRON ENERGY DISTRIBUTION FUNCTION (EEDF)

(Submission paper in progress)

2-components test EEDFs: capturing low-T and high-T properties (**EEDF1** and **EEDF2**)

3-components test EEDFs: low-T + mid-T + high-T properties (**EEDF3** and **EEDF 4**)

Ref. case name	Type
EEDF1	Low-E f_M + High-E f_M
EEDF2	Low-E f_M + High-E f_D
EEDF3	Low-E f_M + Medium-E f_M + High-E f_M
EEDF4	Low-E f_M + Medium-E f_D + High-E f_M

BEST EEDF2: LOW-MAXWELLIAN + HIGH-DRUYVESTEYN

$$f(E,kT_1,kT_2) = N_1\left(\frac{2}{\sqrt{\pi}}\frac{\sqrt{E}}{\sqrt{(kT_1)^3}}e^{-E/kT_1}\right) + N_2\left(1.04\frac{\sqrt{E}}{\sqrt{(kT_2)^3}}e^{-0.55E^2/(kT_2)^2}\right)$$

Qualitative analysis on j-th ROI-aggregated collective data for the i-th energy interval

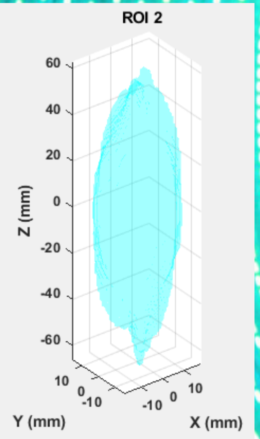

$$(\boldsymbol{\rho}_{ij})_{est} = (\sum_{i=1}^{7}\boldsymbol{\rho}_{ij})\int_a^b f(E;(\mathbf{k_B T}_l)_j;(\mathbf{k_B T}_h)_j)\mathrm{d}E$$

Density Comparison (ROI 2)

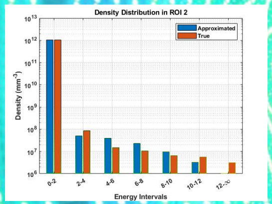

$$(\mathbf{E}_{ij})_{est} = \frac{\int_a^b f(E;(\mathbf{k_B T}_l)_j;(\mathbf{k_B T}_h)_j)E\mathrm{d}E}{\int_a^b f(E;(\mathbf{k_B T}_l)_j;(\mathbf{k_B T}_h)_j)\mathrm{d}E}$$

Fit parameters

$$(\mathrm{k_B T}_l)_j = \frac{2}{3}\mathrm{C}_j\mathrm{E}_{1j}, \quad (\mathrm{k_B T}_h)_j = \mathrm{S}_j\frac{\sum_{i=2}^{7}\rho_{ij}\mathrm{E}_{ij}}{\sum_{i=2}^{7}\rho_{ij}}$$

Fit analysis

$$\langle MSE\rangle_j = \frac{1}{N(j)}\sum_{k(j)=1}^{N(j)} MSE_{k(j)},$$

$$\sigma_{\langle MSE\rangle_j} = \frac{1}{\sqrt{N(j)-1}}\sqrt{\sum_{k(j)=1}^{N(j)}(MSE_{k(j)}-\langle MSE\rangle_j)^2}$$

$$\langle r^2\rangle_j = \frac{1}{N(j)}\sum_{k(j)=1}^{N(j)}(r^2)_{k(j)},$$

$$\sigma_{\langle r^2\rangle_j} = \frac{1}{\sqrt{N(j)-1}}\sqrt{\sum_{k(j)=1}^{N(j)}((r^2)_{k(j)}-\langle r^2\rangle_j)^2}$$

(Submission paper in progress)

2-components test EEDFs: capturing low-T and high-T properties (**EEDF1** and **EEDF2**)

3-components test EEDFs: low-T + mid-T + high-T properties (**EEDF3** and **EEDF 4**)

Ref. case name	Type
EEDF1	Low-E f_M + High-E f_M
EEDF2	Low-E f_M + High-E f_D
EEDF3	Low-E f_M + Medium-E f_M + High-E f_M
EEDF4	Low-E f_M + Medium-E f_D + High-E f_M

BEST EEDF2: LOW-MAXWELLIAN + HIGH-DRUYVESTEYN

$$f(E,kT_1,kT_2) = N_1\left(\frac{2}{\sqrt{\pi}}\frac{\sqrt{E}}{\sqrt{(kT_1)^3}}e^{-E/kT_1}\right) + N_2\left(1.04\frac{\sqrt{E}}{\sqrt{(kT_2)^3}}e^{-0.55E^2/(kT_2)^2}\right)$$

Qualitative analysis on j-th ROI-aggregated collective data for the i-th energy interval

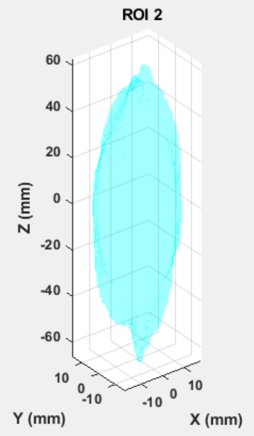

$$(\boldsymbol{\rho}_{ij})_{est} = \left(\sum_{i=1}^{7}\boldsymbol{\rho}_{ij}\right)\int_a^b f(E:(\mathbf{k_B T}_l)_j:(\mathbf{k_B T}_h)_j)\,\mathrm{d}E$$

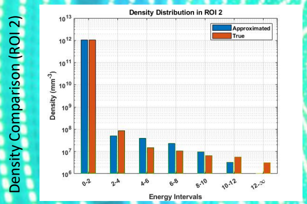

$$(\mathbf{E}_{ij})_{est} = \frac{\int_a^b f(E:(\mathbf{k_B T}_l)_j:(\mathbf{k_B T}_h)_j)E\,\mathrm{d}E}{\int_a^b f(E:(\mathbf{k_B T}_l)_j:(\mathbf{k_B T}_h)_j)\,\mathrm{d}E}$$

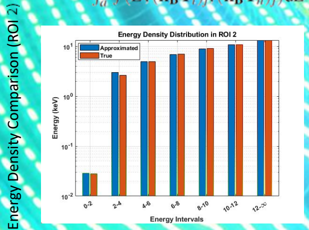

Fit parameters

$$(\mathbf{k_B T}_l)_j = \frac{2}{3}\mathbf{C}_j\mathbf{E}_{1j}, \quad (\mathbf{k_B T}_h)_j = \mathbf{S}_j\frac{\sum_{i=2}^{7}\rho_{ij}\mathbf{E}_{ij}}{\sum_{i=2}^{7}\rho_{ij}}$$

Fit analysis

$$\langle MSE\rangle_j = \frac{1}{N(j)}\sum_{k(j)=1}^{N(j)} MSE_{k(j)},$$

$$\sigma_{\langle MSE\rangle_j} = \frac{1}{\sqrt{N(j)-1}}\sqrt{\sum_{k(j)=1}^{N(j)}(MSE_{k(j)} - \langle MSE\rangle_j)^2}$$

$$\langle r^2\rangle_j = \frac{1}{N(j)}\sum_{k(j)=1}^{N(j)}(r^2)_{k(j)},$$

$$\sigma_{\langle r^2\rangle_j} = \frac{1}{\sqrt{N(j)-1}}\sqrt{\sum_{k(j)=1}^{N(j)}((r^2)_{k(j)} - \langle r^2\rangle_j)^2}$$

<u>SPACE-RESOLVED</u> ELECTRON ENERGY DISTRIBUTION FUNCTION (EEDF)

(Submission paper in progress)

2-components test EEDFs: capturing low-T and high-T properties (**EEDF1** and **EEDF2**)

3-components test EEDFs: low-T + mid-T + high-T properties (**EEDF3** and **EEDF 4**)

Ref. case name	Type
EEDF1	Low-E f_M + High-E f_M
EEDF2	Low-E f_M + High-E f_D
EEDF3	Low-E f_M + Medium-E f_M + High-E f_M
EEDF4	Low-E f_M + Medium-E f_D + High-E f_M

BEST EEDF2: LOW-MAXWELLIAN + HIGH-DRUYVESTEYN

$$f(E,kT_1,kT_2) = N_1\left(\frac{2}{\sqrt{\pi}}\frac{\sqrt{E}}{\sqrt{(kT_1)^3}}e^{-E/kT_1}\right) + N_2\left(1.04\frac{\sqrt{E}}{\sqrt{(kT_2)^3}}e^{-0.55E^2/(kT_2)^2}\right)$$

Qualitative analysis on j-th ROI-aggregated collective data for the i-th energy interval

$$(\boldsymbol{\rho}_{ij})_{est} = (\sum_{i=1}^{7}\boldsymbol{\rho}_{ij})\int_a^b f(E:(\mathbf{k_B T}_l)_j:(\mathbf{k_B T}_h)_j)\mathrm{d}E$$

$$(\mathbf{E}_{ij})_{est} = \frac{\int_a^b f(E:(\mathbf{k_B T}_l)_j:(\mathbf{k_B T}_h)_j)E\mathrm{d}E}{\int_a^b f(E:(\mathbf{k_B T}_l)_j:(\mathbf{k_B T}_h)_j)\mathrm{d}E}$$

Fit parameters

$$(\mathrm{k_B T}_l)_j = \frac{2}{3}\mathrm{C}_j\mathrm{E}_{1j}, \quad (\mathrm{k_B T}_h)_j = \mathrm{S}_j\frac{\sum_{i=2}^{7}\rho_{ij}\mathrm{E}_{ij}}{\sum_{i=2}^{7}\rho_{ij}}$$

Fit analysis

$$\langle MSE\rangle_j = \frac{1}{N(j)}\sum_{k(j)=1}^{N(j)} MSE_{k(j)},$$

$$\sigma_{\langle MSE\rangle_j} = \frac{1}{\sqrt{N(j)-1}}\sqrt{\sum_{k(j)=1}^{N(j)}(MSE_{k(j)} - \langle MSE\rangle_j)^2}$$

$$\langle r^2\rangle_j = \frac{1}{N(j)}\sum_{k(j)=1}^{N(j)}(r^2)_{k(j)},$$

$$\sigma_{\langle r^2\rangle_j} = \frac{1}{\sqrt{N(j)-1}}\sqrt{\sum_{k(j)=1}^{N(j)}((r^2)_{k(j)} - \langle r^2\rangle_j)^2}$$

SPACE-RESOLVED ELECTRON ENERGY DISTRIBUTION FUNCTION (EEDF)

(Submission paper in progress)

Istituto Nazionale di Fisica Nucleare
Laboratori Nazionali del Sud

2-components test EEDFs: capturing low-T and high-T properties (**EEDF1** and **EEDF2**)

3-components test EEDFs: low-T + mid-T + high-T properties (**EEDF3** and **EEDF 4**)

Ref. case name	Type
EEDF1	Low-E f_M + High-E f_M
EEDF2	Low-E f_M + High-E f_D
EEDF3	Low-E f_M + Medium-E f_M + High-E f_M
EEDF4	Low-E f_M + Medium-E f_D + High-E f_M

BEST EEDF2: LOW-MAXWELLIAN + HIGH-DRUYVESTEYN

$$f(E,kT_1,kT_2) = N_1\left(\frac{2}{\sqrt{\pi}}\frac{\sqrt{E}}{\sqrt{(kT_1)^3}}e^{-E/kT_1}\right) + N_2\left(1.04\frac{\sqrt{E}}{\sqrt{(kT_2)^3}}e^{-0.55E^2/(kT_2)^2}\right)$$

Qualitative analysis on j-th ROI-aggregated collective data for the i-th energy interval

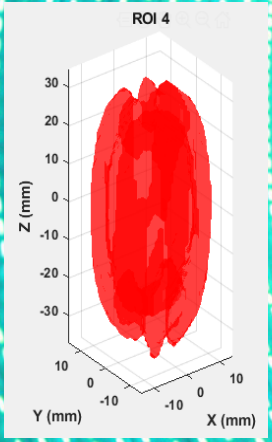

$$(\boldsymbol{\rho}_{ij})_{est} = (\sum_{i=1}^{7}\boldsymbol{\rho}_{ij})\int_a^b f(E;(\mathbf{k_B T}_l)_j;(\mathbf{k_B T}_h)_j)\mathrm{d}E$$

$$(\mathbf{E}_{ij})_{est} = \frac{\int_a^b f(E;(\mathbf{k_B T}_l)_j;(\mathbf{k_B T}_h)_j)E\mathrm{d}E}{\int_a^b f(E;(\mathbf{k_B T}_l)_j;(\mathbf{k_B T}_h)_j)\mathrm{d}E}$$

Fit parameters

$$(\mathbf{k_B T}_l)_j = \frac{2}{3}\mathbf{C}_j\mathbf{E}_{1j}, \quad (\mathbf{k_B T}_h)_j = \mathbf{S}_j\frac{\sum_{i=2}^{7}\boldsymbol{\rho}_{ij}\mathbf{E}_{ij}}{\sum_{i=2}^{7}\boldsymbol{\rho}_{ij}}$$

Fit analysis

$$\langle MSE\rangle_j = \frac{1}{N(j)}\sum_{k(j)=1}^{N(j)} MSE_{k(j)},$$

$$\sigma_{\langle MSE\rangle_j} = \frac{1}{\sqrt{N(j)-1}}\sqrt{\sum_{k(j)=1}^{N(j)}(MSE_{k(j)} - \langle MSE\rangle_j)^2}$$

$$\langle r^2\rangle_j = \frac{1}{N(j)}\sum_{k(j)=1}^{N(j)}(r^2)_{k(j)},$$

$$\sigma_{\langle r^2\rangle_j} = \frac{1}{\sqrt{N(j)-1}}\sqrt{\sum_{k(j)=1}^{N(j)}((r^2)_{k(j)} - \langle r^2\rangle_j)^2}$$

SPACE-RESOLVED ELECTRON ENERGY DISTRIBUTION FUNCTION (EEDF)

(Submission paper in progress)

Ref. case name	Type
EEDF1	Low-E f_M + High-E f_M
EEDF2	Low-E f_M + High-E f_D
EEDF3	Low-E f_M + Medium-E f_M + High-E f_M
EEDF4	Low-E f_M + Medium-E f_D + High-E f_M

2-components test EEDFs: capturing low-T and high-T properties (**EEDF1** and **EEDF2**)

3-components test EEDFs: low-T + mid-T + high-T properties (**EEDF3** and **EEDF 4**)

BEST EEDF2: LOW-MAXWELLIAN + HIGH-DRUYVESTEYN

$$f(E,kT_1,kT_2) = N_1\left(\frac{2}{\sqrt{\pi}}\frac{\sqrt{E}}{\sqrt{(kT_1)^3}}e^{-E/kT_1}\right) + N_2\left(1.04\frac{\sqrt{E}}{\sqrt{(kT_2)^3}}e^{-0.55E^2/(kT_2)^2}\right)$$

Qualitative analysis on j-th ROI-aggregated collective data for the i-th energy interval

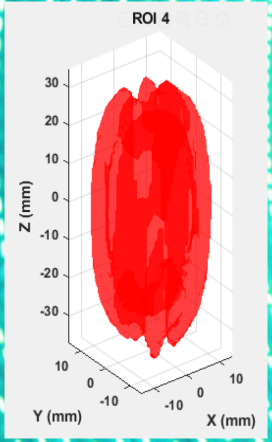

$$(\rho_{ij})_{est} = (\sum_{i=1}^{7}\rho_{ij})\int_a^b f(E;(\mathbf{k_B T}_l)_j;(\mathbf{k_B T}_h)_j)\mathrm{d}E$$

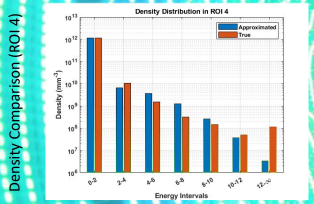

$$(\mathbf{E}_{ij})_{est} = \frac{\int_a^b f(E;(\mathbf{k_B T}_l)_j;(\mathbf{k_B T}_h)_j)E\mathrm{d}E}{\int_a^b f(E;(\mathbf{k_B T}_l)_j;(\mathbf{k_B T}_h)_j)\mathrm{d}E}$$

Fit parameters

$$(\mathbf{k_B T}_l)_j = \frac{2}{3}\mathbf{C}_j\mathbf{E}_{1j}, \quad (\mathbf{k_B T}_h)_j = \mathbf{S}_j\frac{\sum_{i=2}^{7}\rho_{ij}\mathbf{E}_{ij}}{\sum_{i=2}^{7}\rho_{ij}}$$

Fit analysis

$$\langle MSE\rangle_j = \frac{1}{N(j)}\sum_{k(j)=1}^{N(j)} MSE_{k(j)},$$

$$\sigma_{\langle MSE\rangle_j} = \frac{1}{\sqrt{N(j)-1}}\sqrt{\sum_{k(j)=1}^{N(j)}(MSE_{k(j)}-\langle MSE\rangle_j)^2}$$

$$\langle r^2\rangle_j = \frac{1}{N(j)}\sum_{k(j)=1}^{N(j)}(r^2)_{k(j)},$$

$$\sigma_{\langle r^2\rangle_j} = \frac{1}{\sqrt{N(j)-1}}\sqrt{\sum_{k(j)=1}^{N(j)}((r^2)_{k(j)}-\langle r^2\rangle_j)^2}$$

SPACE-RESOLVED ELECTRON ENERGY DISTRIBUTION FUNCTION (EEDF)

(Submission paper in progress)

2-components test EEDFs: capturing low-T and high-T properties (**EEDF1** and **EEDF2**)

3-components test EEDFs: low-T + mid-T + high-T properties (**EEDF3** and **EEDF 4**)

Ref. case name	Type
EEDF1	Low-E f_M + High-E f_M
EEDF2	Low-E f_M + High-E f_D
EEDF3	Low-E f_M + Medium-E f_M + High-E f_M
EEDF4	Low-E f_M + Medium-E f_D + High-E f_M

BEST EEDF2: LOW-MAXWELLIAN + HIGH-DRUYVESTEYN

$$f(E,kT_1,kT_2) = N_1\left(\frac{2}{\sqrt{\pi}}\frac{\sqrt{E}}{\sqrt{(kT_1)^3}}e^{-E/kT_1}\right) + N_2\left(1.04\frac{\sqrt{E}}{\sqrt{(kT_2)^3}}e^{-0.55E^2/(kT_2)^2}\right)$$

Qualitative analysis on j-th ROI-aggregated collective data for the i-th energy interval

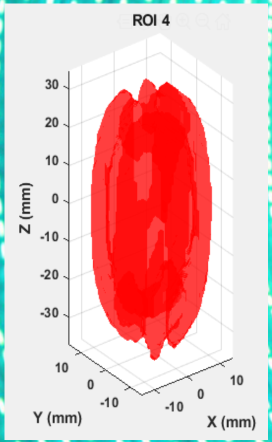

$$(\rho_{ij})_{est} = \left(\sum_{i=1}^{7}\rho_{ij}\right)\int_a^b f(E;(\mathbf{k_B T}_l)_j;(\mathbf{k_B T}_h)_j)\mathrm{d}E$$

Density Comparison (ROI 4)

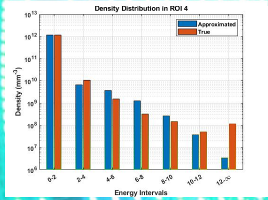

$$(\mathbf{E}_{ij})_{est} = \frac{\int_a^b f(E;(\mathbf{k_B T}_l)_j;(\mathbf{k_B T}_h)_j)E\,\mathrm{d}E}{\int_a^b f(E;(\mathbf{k_B T}_l)_j;(\mathbf{k_B T}_h)_j)\mathrm{d}E}$$

Energy Density Comparison (ROI 4)

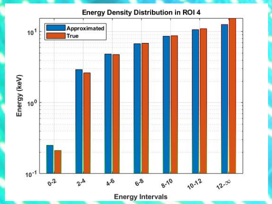

Fit parameters

$$(\mathbf{k_B T}_l)_j = \frac{2}{3}\mathbf{C}_j\mathbf{E}_{1j}, \quad (\mathbf{k_B T}_h)_j = \mathbf{S}_j\frac{\sum_{i=2}^{7}\rho_{ij}\mathbf{E}_{ij}}{\sum_{i=2}^{7}\rho_{ij}}$$

Fit analysis

$$\langle MSE\rangle_j = \frac{1}{N(j)}\sum_{k(j)=1}^{N(j)} MSE_{k(j)},$$

$$\sigma_{\langle MSE\rangle_j} = \frac{1}{\sqrt{N(j)-1}}\sqrt{\sum_{k(j)=1}^{N(j)}(MSE_{k(j)} - \langle MSE\rangle_j)^2}$$

$$\langle r^2\rangle_j = \frac{1}{N(j)}\sum_{k(j)=1}^{N(j)}(r^2)_{k(j)},$$

$$\sigma_{\langle r^2\rangle_j} = \frac{1}{\sqrt{N(j)-1}}\sqrt{\sum_{k(j)=1}^{N(j)}((r^2)_{k(j)} - \langle r^2\rangle_j)^2}$$

SPACE-RESOLVED ELECTRON ENERGY DISTRIBUTION FUNCTION (EEDF)

(Submission paper in progress)

2-components test EEDFs: capturing low-T and high-T properties (**EEDF1** and **EEDF2**)

3-components test EEDFs: low-T + mid-T + high-T properties (**EEDF3** and **EEDF 4**)

Ref. case name	Type
EEDF1	Low-E f_M + High-E f_M
EEDF2	Low-E f_M + High-E f_D
EEDF3	Low-E f_M + Medium-E f_M + High-E f_M
EEDF4	Low-E f_M + Medium-E f_D + High-E f_M

BEST EEDF2: LOW-MAXWELLIAN + HIGH-DRUYVESTEYN

$$f(E,kT_1,kT_2) = N_1\left(\frac{2}{\sqrt{\pi}}\frac{\sqrt{E}}{\sqrt{(kT_1)^3}}e^{-E/kT_1}\right) + N_2\left(1.04\frac{\sqrt{E}}{\sqrt{(kT_2)^3}}e^{-0.55E^2/(kT_2)^2}\right)$$

Qualitative analysis on j-th ROI-aggregated collective data for the i-th energy interval

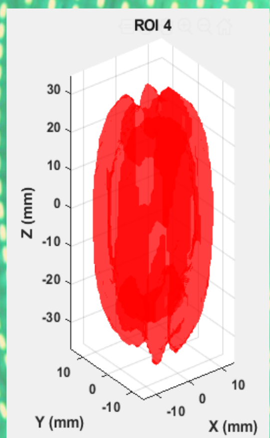

$$(\boldsymbol{\rho}_{ij})_{est} = \left(\sum_{i=1}^{7}\boldsymbol{\rho}_{ij}\right)\int_a^b f(E:(\mathbf{k_B T}_l)_j:(\mathbf{k_B T}_h)_j)\,\mathrm{d}E$$

Density Comparison (ROI 4)

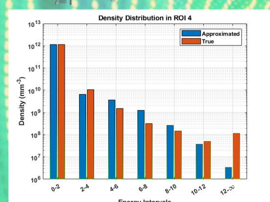

$$(\mathbf{E}_{ij})_{est} = \frac{\int_a^b f(E:(\mathbf{k_B T}_l)_j;(\mathbf{k_B T}_h)_j)E\,\mathrm{d}E}{\int_a^b f(E:(\mathbf{k_B T}_l)_j;(\mathbf{k_B T}_h)_j)\,\mathrm{d}E}$$

Energy Density Comparison (ROI 4)

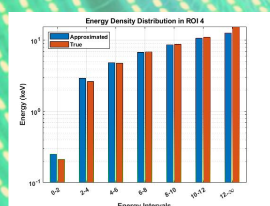

Fit parameters

$$(\mathbf{k_B T}_l)_j = \frac{2}{3}\mathbf{C}_j\mathbf{E}_{1j}, \quad (\mathbf{k_B T}_h)_j = \mathbf{S}_j\frac{\sum_{i=2}^{7}\boldsymbol{\rho}_{ij}\mathbf{E}_{ij}}{\sum_{i=2}^{7}\boldsymbol{\rho}_{ij}}$$

Fit analysis

$$\langle MSE\rangle_j = \frac{1}{N(j)}\sum_{k(j)=1}^{N(j)} MSE_{k(j)},$$

$$\sigma_{\langle MSE\rangle_j} = \frac{1}{\sqrt{N(j)-1}}\sqrt{\sum_{k(j)=1}^{N(j)}(MSE_{k(j)} - \langle MSE\rangle_j)^2}$$

$$\langle r^2\rangle_j = \frac{1}{N(j)}\sum_{k(j)=1}^{N(j)}(r^2)_{k(j)},$$

$$\sigma_{\langle r^2\rangle_j} = \frac{1}{\sqrt{N(j)-1}}\sqrt{\sum_{k(j)=1}^{N(j)}((r^2)_{k(j)} - \langle r^2\rangle_j)^2}$$

SPACE-RESOLVED ELECTRON ENERGY DISTRIBUTION FUNCTION (EEDF)

(Submission paper in progress)

2-components test EEDFs: capturing low-T and high-T properties (**EEDF1** and **EEDF2**)

3-components test EEDFs: low-T + mid-T + high-T properties (**EEDF3** and **EEDF 4**)

Ref. case name	Type
EEDF1	Low-E f_M + High-E f_M
EEDF2	Low-E f_M + High-E f_D
EEDF3	Low-E f_M + Medium-E f_M + High-E f_M
EEDF4	Low-E f_M + Medium-E f_D + High-E f_M

BEST EEDF2: LOW-MAXWELLIAN + HIGH-DRUYVESTEYN

$$f(E, kT_1, kT_2) = N_1\left(\frac{2}{\sqrt{\pi}}\frac{\sqrt{E}}{\sqrt{(kT_1)^3}}e^{-E/kT_1}\right) + N_2\left(1.04\frac{\sqrt{E}}{\sqrt{(kT_2)^3}}e^{-0.55E^2/(kT_2)^2}\right)$$

Quantitative analysis cell-by-cell

Qualitative analysis on j-th ROI-aggregated collective data for the i-th energy interval

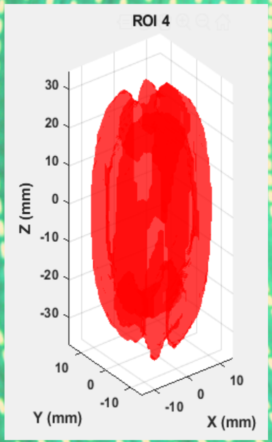

$$(\boldsymbol{\rho}_{ij})_{est} = (\sum_{i=1}^{7}\boldsymbol{\rho}_{ij})\int_a^b f(E;(\mathbf{k_B T}_l)_j;(\mathbf{k_B T}_h)_j)\mathrm{d}E$$

Density Comparison (ROI 4)

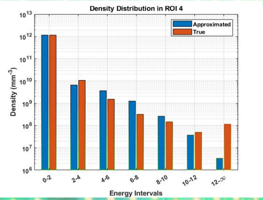

$$(\mathbf{E}_{ij})_{est} = \frac{\int_a^b f(E;(\mathbf{k_B T}_l)_j;(\mathbf{k_B T}_h)_j)E\mathrm{d}E}{\int_a^b f(E;(\mathbf{k_B T}_l)_j;(\mathbf{k_B T}_h)_j)\mathrm{d}E}$$

Energy Density Comparison (ROI 4)

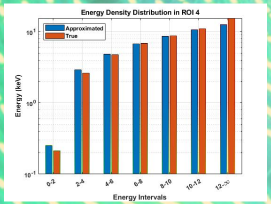

Fit parameters

$$(\mathrm{k_B T}_l)_j = \frac{2}{3}\mathrm{C}_j\mathrm{E}_{1j}, \quad (\mathrm{k_B T}_h)_j = \mathrm{S}_j\frac{\sum_{i=2}^{7}\rho_{ij}\mathrm{E}_{ij}}{\sum_{i=2}^{7}\rho_{ij}}$$

Fit analysis

$$\langle MSE\rangle_j = \frac{1}{N(j)}\sum_{k(j)=1}^{N(j)} MSE_{k(j)},$$

$$\sigma_{\langle MSE\rangle_j} = \frac{1}{\sqrt{N(j)-1}}\sqrt{\sum_{k(j)=1}^{N(j)}(MSE_{k(j)} - \langle MSE\rangle_j)^2}$$

$$\langle r^2\rangle_j = \frac{1}{N(j)}\sum_{k(j)=1}^{N(j)}(r^2)_{k(j)},$$

$$\sigma_{\langle r^2\rangle_j} = \frac{1}{\sqrt{N(j)-1}}\sqrt{\sum_{k(j)=1}^{N(j)}((r^2)_{k(j)} - \langle r^2\rangle_j)^2}$$

SPACE-RESOLVED ELECTRON ENERGY DISTRIBUTION FUNCTION (EEDF)

(Submission paper in progress)

Istituto Nazionale di Fisica Nucleare
Laboratori Nazionali del Sud

2-components test EEDFs: capturing low-T and high-T properties (**EEDF1** and **EEDF2**)
3-components test EEDFs: low-T + mid-T + high-T properties (**EEDF3** and **EEDF 4**)

Ref. case name	Type
EEDF1	Low-E f_M + High-E f_M
EEDF2	Low-E f_M + High-E f_D
EEDF3	Low-E f_M + Medium-E f_M + High-E f_M
EEDF4	Low-E f_M + Medium-E f_D + High-E f_M

BEST EEDF2: LOW-MAXWELLIAN + HIGH-DRUYVESTEYN

$$f(E,kT_1,kT_2) = N_1\left(\frac{2}{\sqrt{\pi}}\frac{\sqrt{E}}{\sqrt{(kT_1)^3}}e^{-E/kT_1}\right) + N_2\left(1.04\frac{\sqrt{E}}{\sqrt{(kT_2)^3}}e^{-0.55E^2/(kT_2)^2}\right)$$

Qualitative analysis on j-th ROI-aggregated collective data for the i-th energy interval

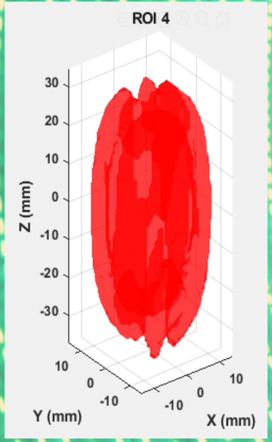

$$(\boldsymbol{\rho}_{ij})_{est} = (\sum_{i=1}^{7}\boldsymbol{\rho}_{ij})\int_a^b f(E:(\mathbf{k_B T}_l)_j:(\mathbf{k_B T}_h)_j)\mathrm{d}E$$

Density Comparison (ROI 4)

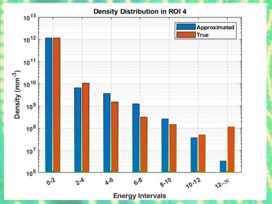

$$(\mathbf{E}_{ij})_{est} = \frac{\int_a^b f(E:(\mathbf{k_B T}_l)_j:(\mathbf{k_B T}_h)_j)E\mathrm{d}E}{\int_a^b f(E:(\mathbf{k_B T}_l)_j:(\mathbf{k_B T}_h)_j)\mathrm{d}E}$$

Energy Density Comparison (ROI 4)

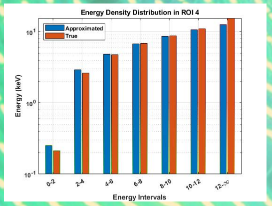

Fit parameters

$$(\mathrm{k_B T}_l)_j = \frac{2}{3}\mathrm{C}_j\mathrm{E}_{1j}, \quad (\mathrm{k_B T}_h)_j = \mathrm{S}_j\frac{\sum_{i=2}^{7}\rho_{ij}\mathrm{E}_{ij}}{\sum_{i=2}^{7}\rho_{ij}}$$

Fit analysis

$$\langle MSE\rangle_j = \frac{1}{N(j)}\sum_{k(j)=1}^{N(j)} MSE_{k(j)},$$

$$\sigma_{\langle MSE\rangle_j} = \frac{1}{\sqrt{N(j)-1}}\sqrt{\sum_{k(j)=1}^{N(j)}(MSE_{k(j)}-\langle MSE\rangle_j)^2}$$

$$\langle r^2\rangle_j = \frac{1}{N(j)}\sum_{k(j)=1}^{N(j)}(r^2)_{k(j)},$$

$$\sigma_{\langle r^2\rangle_j} = \frac{1}{\sqrt{N(j)-1}}\sqrt{\sum_{k(j)=1}^{N(j)}((r^2)_{k(j)}-\langle r^2\rangle_j)^2}$$

Quantitative analysis cell-by-cell

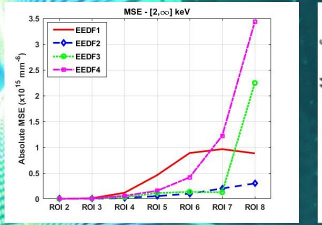

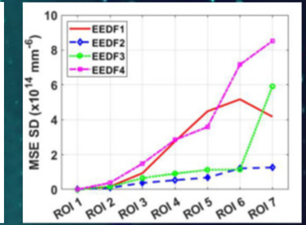

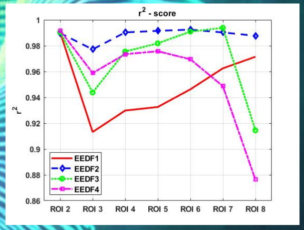

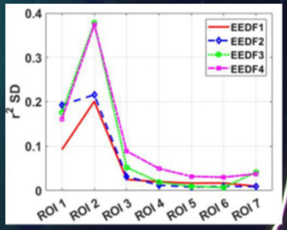

Mean Squared Error and r² Values for different EEDFs in each ROI

SPACE-RESOLVED ELECTRON ENERGY DISTRIBUTION FUNCTION (EEDF)

(Submission paper in progress)

2-components test EEDFs: capturing low-T and high-T properties (**EEDF1** and **EEDF2**)

3-components test EEDFs: low-T + mid-T + high-T properties (**EEDF3** and **EEDF 4**)

Ref. case name	Type
EEDF1	Low-E f_M + High-E f_M
EEDF2	Low-E f_M + High-E f_D
EEDF3	Low-E f_M + Medium-E f_M + High-E f_M
EEDF4	Low-E f_M + Medium-E f_D + High-E f_M

BEST EEDF2: LOW-MAXWELLIAN + HIGH-DRUYVESTEYN

$$f(E, kT_1, kT_2) = N_1\left(\frac{2}{\sqrt{\pi}}\frac{\sqrt{E}}{\sqrt{(kT_1)^3}}e^{-E/kT_1}\right) + N_2\left(1.04\frac{\sqrt{E}}{\sqrt{(kT_2)^3}}e^{-0.55E^2/(kT_2)^2}\right)$$

Qualitative analysis on j-th ROI-aggregated collective data for the i-th energy interval

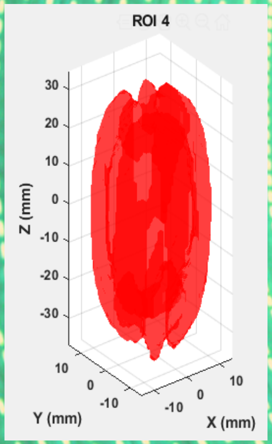

$$(\boldsymbol{\rho}_{ij})_{est} = \left(\sum_{i=1}^{7}\boldsymbol{\rho}_{ij}\right)\int_a^b f(E:(\mathbf{k_B T}_l)_j:(\mathbf{k_B T}_h)_j)\mathrm{d}E$$

Density Comparison (ROI 4)

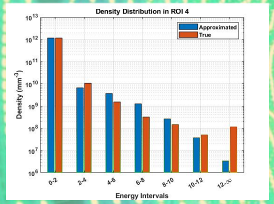

$$(\mathbf{E}_{ij})_{est} = \frac{\int_a^b f(E:(\mathbf{k_B T}_l)_j:(\mathbf{k_B T}_h)_j)E\mathrm{d}E}{\int_a^b f(E:(\mathbf{k_B T}_l)_j:(\mathbf{k_B T}_h)_j)\mathrm{d}E}$$

Energy Density Comparison (ROI 4)

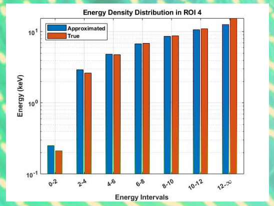

Fit parameters

$$(\mathbf{k_B T}_l)_j = \frac{2}{3}\mathbf{C}_j\mathbf{E}_{1j}, \quad (\mathbf{k_B T}_h)_j = \mathbf{S}_j\frac{\sum_{i=2}^{7}\rho_{ij}\mathbf{E}_{ij}}{\sum_{i=2}^{7}\rho_{ij}}$$

Fit analysis

$$\langle MSE\rangle_j = \frac{1}{N(j)}\sum_{k(j)=1}^{N(j)} MSE_{k(j)},$$

$$\sigma_{\langle MSE\rangle_j} = \frac{1}{\sqrt{N(j)-1}}\sqrt{\sum_{k(j)=1}^{N(j)}(MSE_{k(j)} - \langle MSE\rangle_j)^2}$$

$$\langle r^2\rangle_j = \frac{1}{N(j)}\sum_{k(j)=1}^{N(j)}(r^2)_{k(j)},$$

$$\sigma_{\langle r^2\rangle_j} = \frac{1}{\sqrt{N(j)-1}}\sqrt{\sum_{k(j)=1}^{N(j)}((r^2)_{k(j)} - \langle r^2\rangle_j)^2}$$

Quantitative analysis cell-by-cell

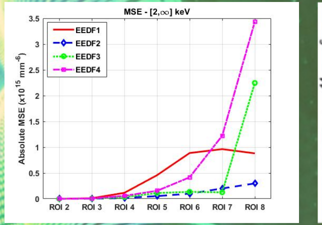

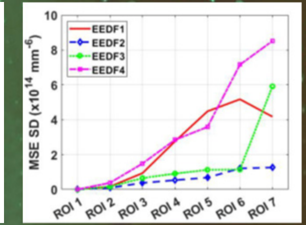

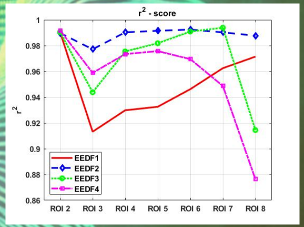

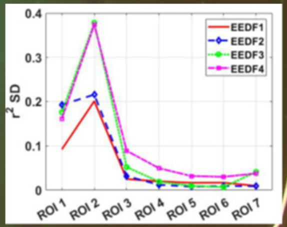

Mean Squared Error and r^2 Values for different EEDFs in each ROI

1st EEDF TEST BENCH: ESTIMATE OF Ar FLUORESCENCE K-α EMISSION

Argon plasma **emission rate** for the **K-shell X-ray fluorescence** at **2.96 keV** supporting the **experimental campaign** carried out jointly by the ATOMKI (Debrecen) and INFN-LNS/LNL groups in 2017 on **space-resolved X-ray spectroscopy**

$$R = \rho_e \rho_{Ar} \int_0^\infty \sigma(E) v(E) f(E) dE$$

EXPERIMENTAL SETUP

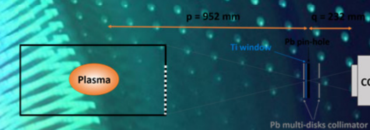

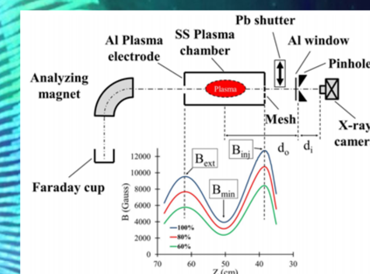

- **Electron data** from simulations used to **evaluate** a **3D K-α emission rate map : using** the **analytical EEDF**
- Geometrical efficiency of detecting system, quantum efficiency of CCD camera and exposure time considered for the emission map

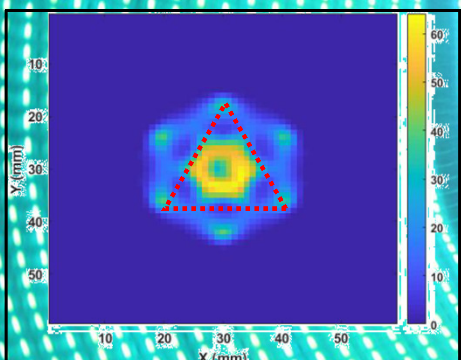

Longitudinally integrated estimated K-α map at the CCD, considering Total Emission, LGE and Quantum Efficiency

B. Mishra, *Master Thesis work (2020)*

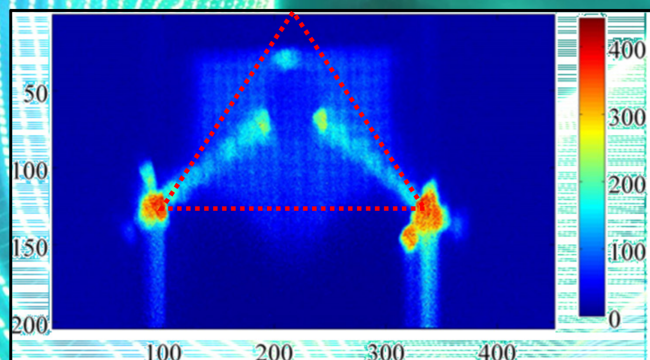

Plot of experimental photon counted images

R. Ràcz *et al.*, PSST 26 (2017) 075011

Numerical emission map not too far from capturing the true physical experimental emission image**: robustness of the evaluated EEDF**

2nd EEDF TEST BENCH: ESTIMATE OF ION CHARGE STATE DISTRIBUTION

ROI	$N_e(cm^{-3})$	N_1	$kT_1(eV)$	N_2	$kT_2(keV)$
1	0	0	–	0	–
2	$4.9362E+11$	0.9998	19.0	0.0002	4.2142
3	$6.8247E+12$	0.9945	109.9	0.0055	3.0010
4	$1.1403E+13$	0.9849	164.7	0.0151	3.1882
5	$1.1649E+13$	0.9695	227.2	0.0305	3.2394
6	$1.0773E+13$	0.9464	292.6	0.0536	3.3766
7	$1.0266E+13$	0.9239	352.0	0.0761	3.5833
8	$9.9190E+12$	0.9033	414.6	0.0967	3.7490

2nd EEDF TEST BENCH: ESTIMATE OF ION CHARGE STATE DISTRIBUTION

ROI	$N_e(cm^{-3})$	N_1	$kT_1(eV)$	N_2	$kT_2(keV)$
1	0	0	–	0	–
2	$4.9362E+11$	0.9998	19.0	0.0002	4.2142
3	$6.8247E+12$	0.9945	109.9	0.0055	3.0010
4	$1.1403E+13$	0.9849	164.7	0.0151	3.1882
5	$1.1649E+13$	0.9695	227.2	0.0305	3.2394
6	$1.0773E+13$	0.9464	292.6	0.0536	3.3766
7	$1.0266E+13$	0.9239	352.0	0.0761	3.5833
8	$9.9190E+12$	0.9033	414.6	0.0967	3.7490

- **Ion CSD** calculated in **spatially-aggregated ROI cells** treated as **0D plasma cell:** 0D code suite **FLYCHK***

***H.K. Chung, R.W. Lee,M.H. Chen and Y. Ralchenko, The How To For FLYCHK @ NIST (2008).**

- **Data input: plasma density + EEDF**

2nd EEDF TEST BENCH: ESTIMATE OF ION CHARGE STATE DISTRIBUTION

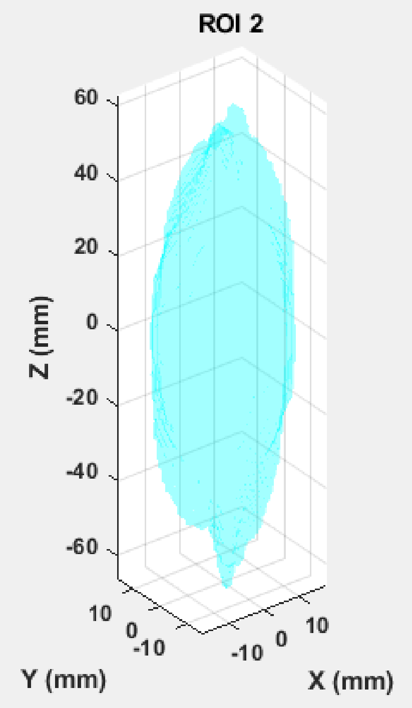

ROI	$N_e(cm^{-3})$	N_1	$kT_1(eV)$	N_2	$kT_2(keV)$
1	0	0	–	0	–
2	$4.9362E+11$	0.9998	19.0	0.0002	4.2142
3	$6.8247E+12$	0.9945	109.9	0.0055	3.0010
4	$1.1403E+13$	0.9849	164.7	0.0151	3.1882
5	$1.1649E+13$	0.9695	227.2	0.0305	3.2394
6	$1.0773E+13$	0.9464	292.6	0.0536	3.3766
7	$1.0266E+13$	0.9239	352.0	0.0761	3.5833
8	$9.9190E+12$	0.9033	414.6	0.0967	3.7490

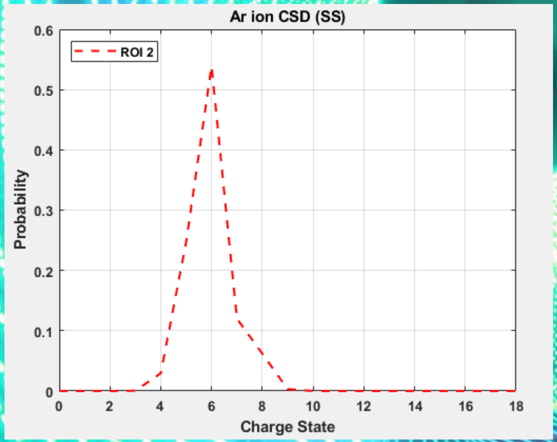

- **Ion CSD** calculated in **spatially-aggregated ROI cells** treated as **0D plasma cell:** 0D code suite **FLYCHK***

*H.K. Chung, R.W. Lee, M.H. Chen and Y. Ralchenko, The How To For FLYCHK @ NIST (2008).

- **Data input: plasma density + EEDF**

2nd EEDF TEST BENCH: ESTIMATE OF ION CHARGE STATE DISTRIBUTION

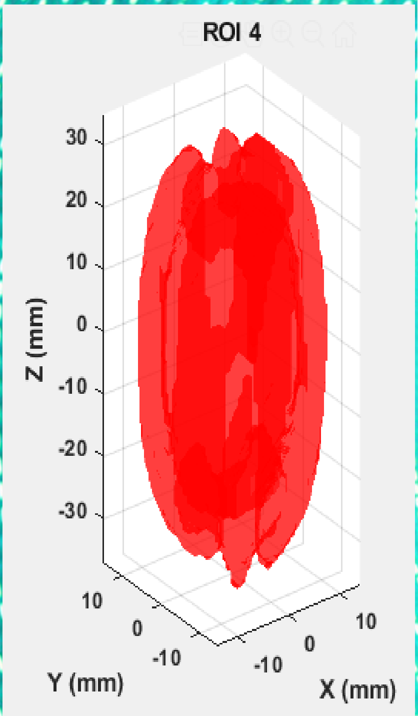

ROI	$N_e(cm^{-3})$	N_1	$kT_1(eV)$	N_2	$kT_2(keV)$
1	0	0	–	0	–
2	$4.9362E+11$	0.9998	19.0	0.0002	4.2142
3	$6.8247E+12$	0.9945	109.9	0.0055	3.0010
4	$1.1403E+13$	0.9849	164.7	0.0151	3.1882
5	$1.1649E+13$	0.9695	227.2	0.0305	3.2394
6	$1.0773E+13$	0.9464	292.6	0.0536	3.3766
7	$1.0266E+13$	0.9239	352.0	0.0761	3.5833
8	$9.9190E+12$	0.9033	414.6	0.0967	3.7490

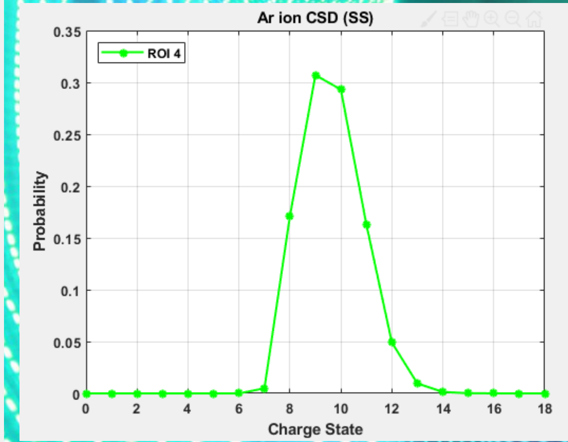

B. Mishra, *Master Thesis work (2020)*

- **Ion CSD** calculated in **spatially-aggregated ROI cells** treated as **0D plasma cell:** 0D code suite **FLYCHK***

*H.K. Chung, R.W. Lee, M.H. Chen and Y. Ralchenko, The How To For FLYCHK @ NIST (2008).

- **Data input: plasma density + EEDF**

2nd EEDF TEST BENCH: ESTIMATE OF ION CHARGE STATE DISTRIBUTION

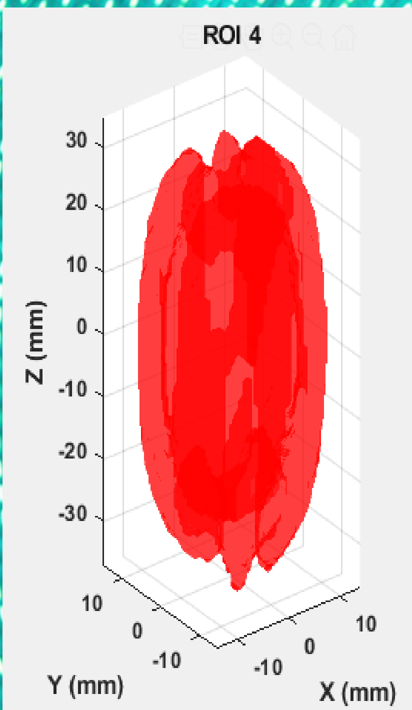

ROI	$N_e(cm^{-3})$	N_1	$kT_1(eV)$	N_2	$kT_2(keV)$
1	0	0	–	0	–
2	$4.9362E+11$	0.9998	19.0	0.0002	4.2142
3	$6.8247E+12$	0.9945	109.9	0.0055	3.0010
4	$1.1403E+13$	0.9849	164.7	0.0151	3.1882
5	$1.1649E+13$	0.9695	227.2	0.0305	3.2394
6	$1.0773E+13$	0.9464	292.6	0.0536	3.3766
7	$1.0266E+13$	0.9239	352.0	0.0761	3.5833
8	$9.9190E+12$	0.9033	414.6	0.0967	3.7490

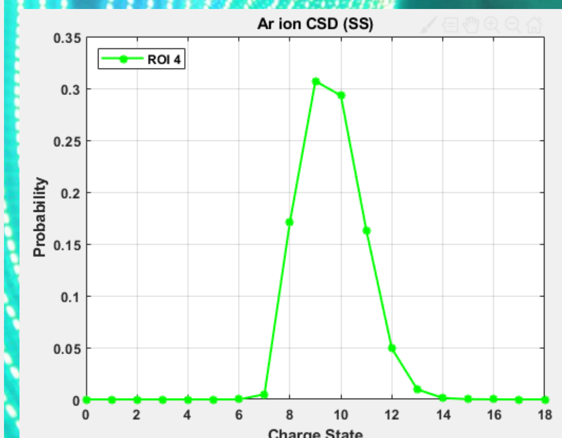

B. Mishra, *Master Thesis work (2020)*

- **Ion CSD** calculated in **spatially-aggregated ROI cells** treated as **0D plasma cell:** 0D code suite **FLYCHK***

*H.K. Chung, R.W. Lee, M.H. Chen and Y. Ralchenko, The How To For FLYCHK @ NIST (2008).

- **Data input: plasma density + EEDF**

- **Higher electron energy content shifts the ion CSD to higher charge states**
- Possibility to use the **0D CSD for 3D modeling** ion-electron dynamics

CONCLUSION

- Self-consistent numerical modeling of ECRIS plasma to study space-resolved and time-resolved phenomena
- Space-resolved particles' anisotropy in the the velocity space reflects the inhomogenous and space-dependent properties of ECRIS plasma
- Space-resolved EEDF provides a local information on the electron distribution
- 2 test bench for the analytical EEDF: 3D map of the fluorescence X-ray emission rate compared with experimental results, evaluation of local ion charge state distribution

ACKNOWLEDGMENTS

INFN LNS
David Mascali
Bharat Mishra
Eugenia Naselli
Giuseppe Torrisi

INFN LNL
Alessio Galatà

CONCLUSION

INFN LNS
Istituto Nazionale di Fisica Nucleare
Laboratori Nazionali del Sud

- Self-consistent numerical modeling of ECRIS plasma to study space-resolved and time-resolved phenomena
- Space-resolved particles' anisotropy in the the velocity space reflects the inhomogenous and space-dependent properties of ECRIS plasma
- Space-resolved EEDF provides a local information on the electron distribution
- 2 test bench for the analytical EEDF: 3D map of the fluorescence X-ray emission rate compared with experimental results, evaluation of local ion charge state distribution

ACKNOWLEDGMENTS

INFN LNS Istituto Nazionale di Fisica Nucleare Laboratori Nazionali del Sud

David Mascali
Bharat Mishra
Eugenia Naselli
Giuseppe Torrisi

INFN LNL Istituto Nazionale di Fisica Nucleare Laboratori Nazionali di Legnaro

Alessio Galatà

THANK YOU ALL !